and vivo. The androgen-independent, androgen receptor-negative rat prostate cancer cell line (PLS10), which was established in our laboratory from a 3,2′-dimethyl-4-aminobiphenyl plus testosterone-induced carcinoma in the dorsolateral prostate of a male F344 rat (Nakanishi et al., 1996), was employed for this purpose.

2. Materials and methods

2.1. Cell culture

The PLS10 cell line was cultured in Roswell Park Memorial Institute-1640 Medium (RPMI 1640, Gibco, Carlsbad, CA) with 10% fetal bovine serum (FBS), 50 U/ml penicillin and 50 μg/ml streptomycin, in a humidified incubator with an atmosphere comprising 95% air and 5% CO_2 at 37 °C.

2.2. Animals

All animal experiments were performed under protocols approved by the Institutional Animal Care and Use Committee of Nagoya City University Graduate School of Medical Sciences. Seven-week-old male athymic nude mice (KSN strain) were purchased from Nihon SLC (Hamamatsu, Japan) and housed in plastic cages with hardwood chip bedding in an air-conditioned room at 23 ± 2 °C and 55 ± 5% humidity with a 12 h light/dark cycle. Oriental MF powder diet (Oriental Yeast Co., Tokyo, Japan) and distilled water were available ad libitum.

2.3. Proliferation assay

PLS10 cells were plated at 2.0×10^2 cells per well in 96-well plates. Twenty-four hours after plating, increasing concentrations of apocynin or NSC23766 (Rac1 inhibitor, COSMO BIO Co., Ltd., Tokyo, Japan) were added. The cells were then incubated for 48 h at 37 °C. Cells cultures were observed microscopically and overall cell number/viability was assessed by WST-1 colorimetric assay (Roche Diagnostics, Mannheim, Germany).

2.4. Cell cycle analysis

After starved conditions with 1% bovine serum albumin instead of 10% FBS, the cells were treated with 250 or 500 μM of apocynin for 48 h, then suspensions were prepared and stained with propidium iodide (Guava® cell cycle reagent, Guava Technologies, Hayward, CA) according to the Guava® Cell Cycle Assay protocol. Cell cycle phase distributions were determined on a Guava® PCA Instrument using CytoSoft Software.

2.5. Invasion assay

For invasion assays, cells were seeded in BD Biocoat™ Matrigel™ invasion chambers (BD Biosciences, San Jose, CA), and treated with apocynin (0, 100 and 200 μM) for 24 h 5% FBS was used as a chemoattractant. Invading cells were fixed with 100% ethanol for 5 min, then stained with 0.5% crystal violet in 20% methanol for 30 min. The number of infiltrating cells was counted under a microscope.

2.6. Detection of ROS production

ROS production was detected by a slightly modification of the method described in a previous report (Rosenkranz et al., 1992). Briefly, 24 h after apocynin treatment, culture supernatant was removed from all wells and the cells were washed twice with warm PBS, then 100 μl of 2′,7′-dichlorofluorescin-diacetate (100 μg/ml, DCFH-DA, Sigma) was added with further incubation at 37 °C for 60 min; in the dark. The cells were washed 3 times with warm PBS, and then were lysed in 100 μl of 2.5% TrironX100. After incubation for 5 min, fluorescence intensity was assessed at 485/535 nm with a spectrofluorometer. Images were also recorded with a fluorescence microscope (BZ-9000; Keyence Corp., Osaka, Japan).

2.7. Detection of vascular endothelial growth factor (VEGF) secretion into the medium

PLS10 cells were plated at 6.0×10^4 cells per well in 24-well plate. Twenty-four hours after plating, they were treated with apocynin or NSC23766 for 24 h. The culture medium of each well was transfered to wells of a Rat VEGF Quantikine ELISA Kit (R&D Systems, Inc., Minneapolis, MN), and VEGF secretion into the medium was determined according to the manufacturer's instructions.

2.8. Immunoblot analyses

After treatment of apocynin or NSC23766, cells were washed with ice-cold phosphate buffer saline (PBS) and scraped with a cell scraper into RIPA buffer (Pierce Biotechnology, Rockford, IL) containing a protease inhibitor (Pierce Biotechnology) on ice. The insoluble matter was removed by centrifugation at 12,000 rpm for 20 min at 4 °C and supernatants were collected. Protein concentrations were determined with a Coomassie Plus™-The Better Bradford Assay Kit (Pierce Biotechnology). Samples were mixed with 2× sample buffer (Bio-Rad Laboratories, Hercules, CA) and heated for 5 min at 95 °C and then subjected to 10% SDS-PAGE. The separated proteins were transferred onto nitrocellulose membranes followed by blocking with SuperBlock Blocking Buffer (Thermo Fisher Scientific K.K., Yokohama, Japan) for 1 h at room temperature. Membranes were probed with antibodies for cyclin D1 (Santa Cruz Biotechnology, Inc., Santa Cruz, CA), cleaved caspase-3, Nuclear Factor Kappa B (NF-κB) p65 and phospho-NF-κB p65 (Ser536) (Cell Signaling, Technology Inc., Danvers, MA), Rac1 (Millipore Corporation, Billerica, MA) and phospho-Rac1 (Upstate, Temecula, CA) in 1× TBS with 0.1% Tween-20 at 4 °C overnight, followed by exposure to peroxidase-conjugated appropriate secondary antibodies and visualization with an enhanced chemiluminescence detection system (GE Healthcare Bio-sciences, Buckinghamshire, NA, UK). To confirm equal protein loading, each membrane was stripped and reprobed with anti-β-actin (Sigma–Aldrich, Co., St. Louis, MO). Band densities of cyclin D1, phospho-NF-κB p65 and phospho-Rac1 were then determined with ImageJ 1.410 (National Institute of Mental Health, MD).

2.9. PLS10 xenograft model

After one week of acclimation, mice were divided into 3 groups of 10 mice each. Two hundred thousand of PLS10 cells were mixed with 50% Matrigel (BD Biosciences) and injected (100 μL) subcutaneously into the back area of each mouse. The animals were given drinking water containing 0, 100 and 500 mg/L apocynin for 30 days and body weights and water consumption were estimated every week. The tumor volumes in each mouse were estimated every other day using the following formula: 0.52 (long axis × short axis × short axis). Mice were sacrificed at experimental day 30, when primary tumors and liver, lung, kidneys and lymph nodes were removed and fixed in 10% buffered formalin. Primary tumors were measured and tumor volume was calculated using the following formula: 0.52 (axis1 × axis2 × axis3). At least 1 section of each tissue and the largest section from each lobe of the lung were processed for hematoxylin and eosin staining, immunostaining and

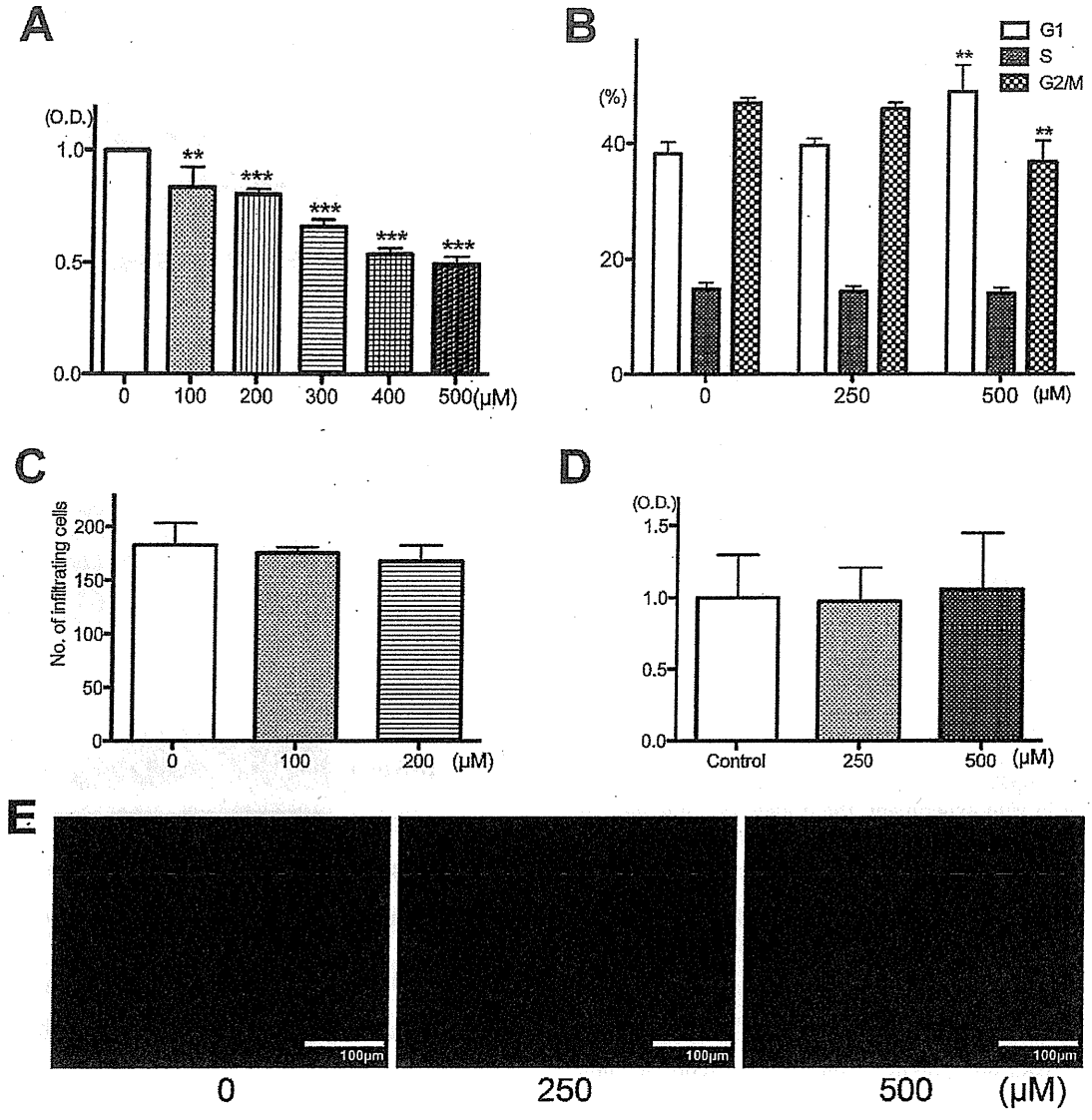

Fig. 1. Apocynin inhibition of cell growth and blockage of cell cycling of PLS10 cells. Cells were incubated with apocynin for 48 h and then cytotoxicity was assessed by WST-1 assay (A). Cell cycle distribution of PLS10 cells after treatment with apocynin for 48 h (B). Cells were treated with 0, 100 and 200 μM apocynin for invasion assays (24 h) using transwell cell culture chambers, with 5% FBS as a chemoattractant (C). ROS production data (D) and photos (E) detected by DCFH-DA after apocynin treatment for 24 h. Data are mean ± SD values from 3 independent experiments. **, ***$P < 0.01$ and 0.001 compared to controls, respectively.

terminal deoxy nucleotidyl transferase-mediated dUTP nick end labeling (TUNEL) assay.

2.10. Immunohistochemistry

Paraffin-embedded specimens were sectioned (3 mm) and stained with Ki67 antibody (SP6; Acris Antibodies GmbH, Herford, Germany), CD31 (Abcam plc, Cambridge, UK), 8-hydroxy-2′-deoxyguanosine (8-OHdG; Nikken SEIL Co., Ltd., Shizuoka, Japan) or Vascular Endothelial Growth Factor (VEGF; Immuno-Biological Laboratories Co., Ltd., Fujioka, Gunma) and then with anti-mouse or -rabbit secondary antibody and avidin–biotin complex (Vectastatin Elite ABC kit; Vector Laboratory, Burlingame, CA), and binding sites were visualized with diamino-benzidine. The sections were then counterstained lightly with hematoxylin for microscopic examination. Staining intensity for VEGF without hematoxylin staining was quantitatively assessed with an Image Processor for Analytical Pathology (IPAP-WIN, Sumika Technos Co., Osaka, Japan) to give optical densities.

2.11. TUNEL assay

Paraffin-embedded specimens were sectioned (3 mm), and apoptotic cells in the tumors were detected by TUNEL assay performed using an In Situ Apoptosis Detection Kit from Takara (Otsu, Japan).

2.12. Statistical analysis

All in vitro experiments were performed at least in triplicate to confirm reproducibility. Statistical analyses were performed with mean ± S.D. values using one-way ANOVA, the Bonferroni correction or Dunnett's test. Statistical significance was concluded at *$P < 0.05$, **$P < 0.01$ or ***$P < 0.001$.

3. Results

WST-1 assay (Fig. 1A) showed that apocynin treatment reduced cell growth of PLS10 cells concentration-dependently after 48 h. At concentrations higher than 100 μM, apocynin treatment significantly inhibited growth, with an inhibitory concentration (IC) 50 of around 500 μM. To explore the underlying mechanism of apocynin-induced growth suppression, cell cycle analysis was performed by Guava® cell cycle assay. Apocynin-treated cells appeared to accumulate in G1 phase, especially at 500 μM (49%, $p < 0.01$), compared to controls (38%), with concomitant decrease in the percentage of cells in the G2/M phase (Fig. 1B). Meanwhile, no significant difference in infiltrating cell number was apparent with/without apocynin treatment in invasion assay (Fig. 1C). Data and photos of ROS detection are presented in Fig. 1D and 1E, respectively. Surprisingly, no significant difference was detected with/without apocynin treatment. Therefore, we investigated another function of the NADPH oxidase complex, and focused on the included Rac1 protein.

Data for expression of Rac-1 and phospho-Rac1 are presented in Fig. 2A. Apocynin treatment only reduced phosphorylation of Rac1 concentration-dependently, but not expression of Rac1. Therefore, we utilized NSC23766, a Rac1 inhibitor, for growth inhibition of PLS10 cells. WST-1 assays indicated that NSC23766 treatment reduced cell growth concentration-dependently after 48 h. At concentrations higher than 10 μM, NSC23766 treatment significantly inhibited growth, with an IC 50 around 200 μM. In the Western blot analysis, both apocynin (500 μM) and NSC23766 (200 μM) treatments reduced phosphorylation of Rac1 and NF-κB p65, and expression of cyclin D1 (Fig. 2C).

During the in vivo experiment, there were no differences in body weight and water consumption among groups (body weight: control, 100 and 500 mg/L apocynin: 27.6 ± 1.8, 27.6 ± 1.6 and 28.4 ± 1.1 g, respectively; water consumption: control, 100 and 500 mg/L apocynin: 4.1 ± 0.2, 4.2 ± 0.2 and 4.1 ± 0.2 ml/mouse/day, respectively). One mouse treated with 500 mg/L apocynin was excluded from the experiment because of spontaneous development of a malignant lymphoma. No toxicity was histologically detected in livers and kidneys of apocynin-treated groups (data not shown), but growth of implanted tumor tended to be reduced (Fig. 3A). Size data and photos of implanted tumors are presented in Fig. 2B and 2C, respectively. Because of individual differences in tumor size, there was no significantly difference between control and apocynin treatment groups overall, but significant reduction was noted with dose-dependence (Spearman's rank correlation coefficient: rho = −0.40, $P < 0.05$). The significant difference between control and 500 mg/L apocynin treatment group was only detected by student T test ($P = 0.0399$). Ki67 labeling indices (Fig. 3D) were significantly reduced by apocynin treatment (100 and 500 mg/L apocynin: 87.7, 86.8%, respectively) in a dose-dependent manner compared to control (90.9%), but TUNEL (Fig. 3E) apoptotic indices were not (control, 100 and 500 mg/L apocynin: 0.88, 0.87 and 0.88%, respectively). To determine antioxidant effects, we investigated the 8-OHdG labeling index (Fig. 3F) but administration of apocynin had no effect (control, 100 and 500 mg/L apocynin: 4.7, 5.0 and 3.8%, respectively). Data for metastatic tumors detected in lungs and/or lymph nodes are presented in Table 1. Apocynin treatment tended to decrease metastatic tumors, but not significantly.

Because reduction of proliferation by apocynin treatment in vivo was relatively slight, we focused on angiogenesis in tumors. Photos and data for numbers of vessels detected with CD31 antibodies are presented in Fig. 4A and B, respectively. The number of vessels per unit tumor area was significantly reduced by apocynin treatment (100 and 500 mg/L apocynin: 185 and 158 mm^{-2}, respectively) compared to control (220 mm^{-2}) with dose-dependence

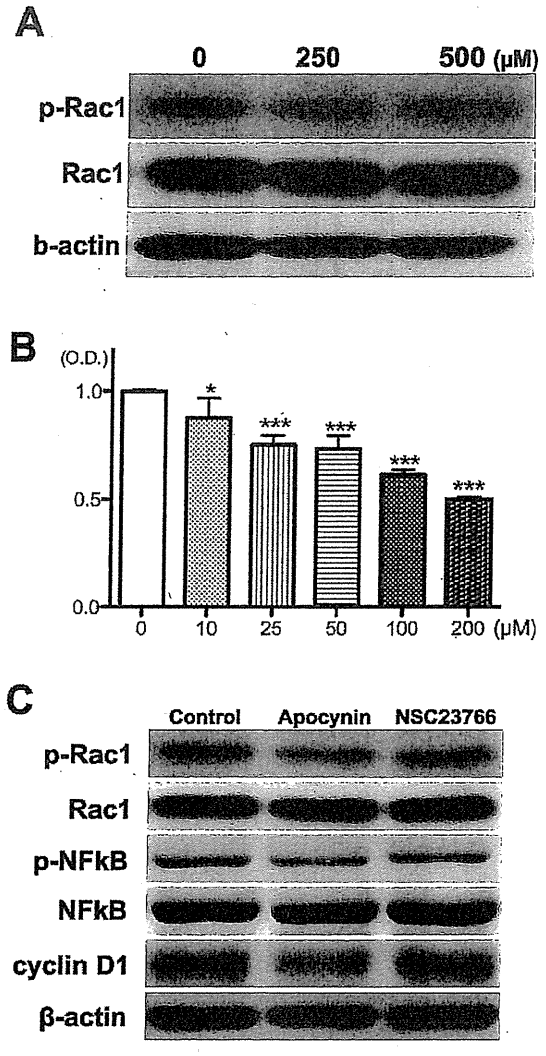

Fig. 2. Apocynin inhibition of phospho-Rac1 in PLS 10 cells. Immunoblot analysis of the protein levels of phosho-Rac1 (p-Rac1), Rac1 and ß-actin (A) with apocynin treatment. The cells were incubated with NSC23766 for 48 h and then cytotoxicity was assessed by WST-1 assay (B). Immunoblot analysis of the protein levels of phosho-Rac1 (p-Rac1), Rac1, phospho-NF-κB (pNF-κB), NF-κB, cyclin D1 and ß-actin (C) with apocynin or NSC23766 treatment. *, ***$P < 0.05$ and 0.001, respectively, compared to 0 μM.

(Spearman's rank correlation coefficient: rho = −0.78, $P < 0.001$). Interestingly, a correlation between tumor size and vessels per tumor was also significant by Spearman's rank correlation coefficient: (rho = 0.52, $P < 0.01$) among all groups. VEGF expression tumor detected by immunostaining was also reduced by apocynin treatment (control, 100 and 500 mg/L apocynin: 1.00, 0.60 and 0.47 optical density, respectively) in a dose-dependent manner (Spearman's rank correlation coefficient: rho = −0.45, $P < 0.05$). In vitro, VEGF secretion from PLS10 cells was significantly reduced by both apocynin and NSC23766 treatments (Fig. 4D).

4. Discussion

In the present study, we demonstrated suppressive effects of apocynin treatment on androgen-independent prostate cancer growth in vitro. Surprisingly, we detected no obvious influence on ROS production but down-regulation of phosphorylated-Rac1 was noted with apocynin treatment, and inhibitory effects were

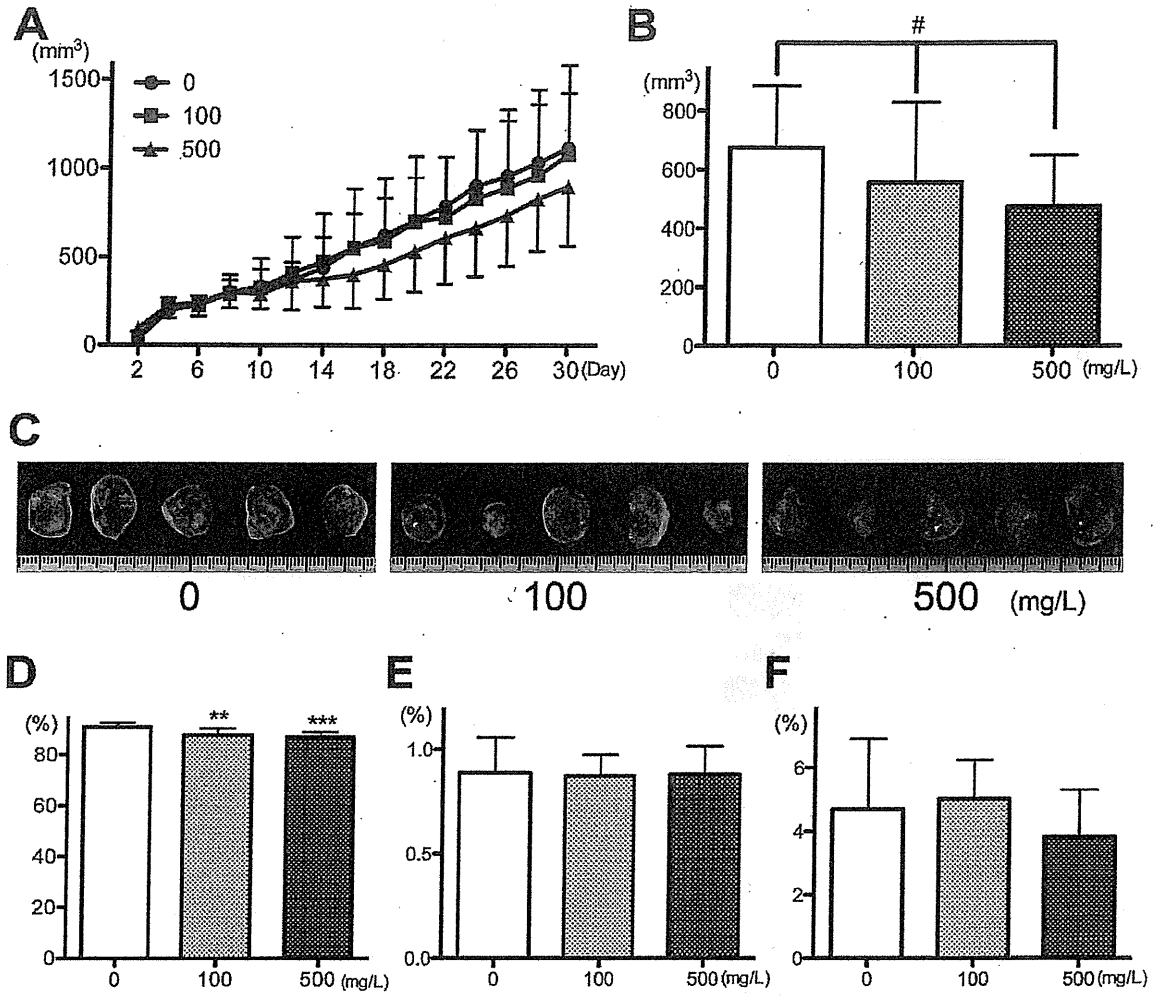

Fig. 3. Apocynin suppression of tumor growth in a PLS10 xenograft model. Nude mice given apocynin (0, 100 and 500 mg/L) in their water were injected subcutaneously with PLS10 cells (2×10^5/animal) into their posterior areas, then sacrificed at day 30. Tumor growth curves (A), data of final tumor size (B), macro photos of tumor (C), Ki67 labeling index (D), percent of TUNEL positive cells (E) and 8-OHdG labeling index are shown. #Spearman's rank correlation coefficient: rho = −0.40, $P < 0.05$, **, ***$P < 0.01$ and 0.001 compared to 0 mg/L, respectively.

confirmed using a Rac1 inhibitor. Rac is a part of the NADPH oxidase complex (Bedard and Krause, 2007), and activated Rac induces NADPH oxidase assembly and activity (Bokoch and Diebold, 2002; Hordijk, 2006). Apocynin is known to block NADPH oxidase assembly (Stolk et al., 1994), and this may be because of reduction of Rac1 activity. More detailed studies are needed to elucidate the mechanism of blocking Rac1 phosphorylation by apocynin.

Concerning human androgen-independent prostate cancer, Kobayashi et al. (2010) demonstrated that activation of Rac1 is related to cell proliferation and androgen-independence. Therefore, the Rac1-regulated pathway appears to be one of the most important for both human and rat androgen-independent prostate cancers, and also an anti-tumor target with apocynin. A number of reports have indicated that prostate cancer cells generate substantial amounts of ROS which are related to cell growth and malignant potential (Kumar et al., 2008; Khandrika et al., 2009). In particular, Kumar et al. (2008) described that another NADPH oxidase inhibitor, diphenyleneiodonium, had the ability to block both ROS production and aggressive potential in some prostate cancer cell lines in vitro.

In vivo, we demonstrated inhibition of implanted tumor growth by apocynin treatment, with reduction of metastatic tumors in lungs and lymph nodes. The dose of apocynin administrated to mice did not cause toxicity, as there were no effects on body weight or water consumption. Interestingly, the inhibitory mechanisms of tumor growth by apocynin appeared related not only with direct effects on cell proliferation but also angiogenesis, as evidenced by decrease of vessels and expression and secretion of

Table 1
Incidence and multiplicity of metastatic tumors in lungs and lymph nodes of xgenograft model.

Treatment	Animal No.	Lung metastasis		Lymph node metastasis	
		Incidence	Multiplicity	Incidence	Multiplicity
Control	10	7	1.40 ± 1.78	2	0.20 ± 0.42
Apocynin 100 mg/L	10	3	0.60 ± 1.07	2	0.20 ± 0.42
Apocynin 500 mg/L	9	3	0.44 ± 0.73	0	0.00 ± 0.00

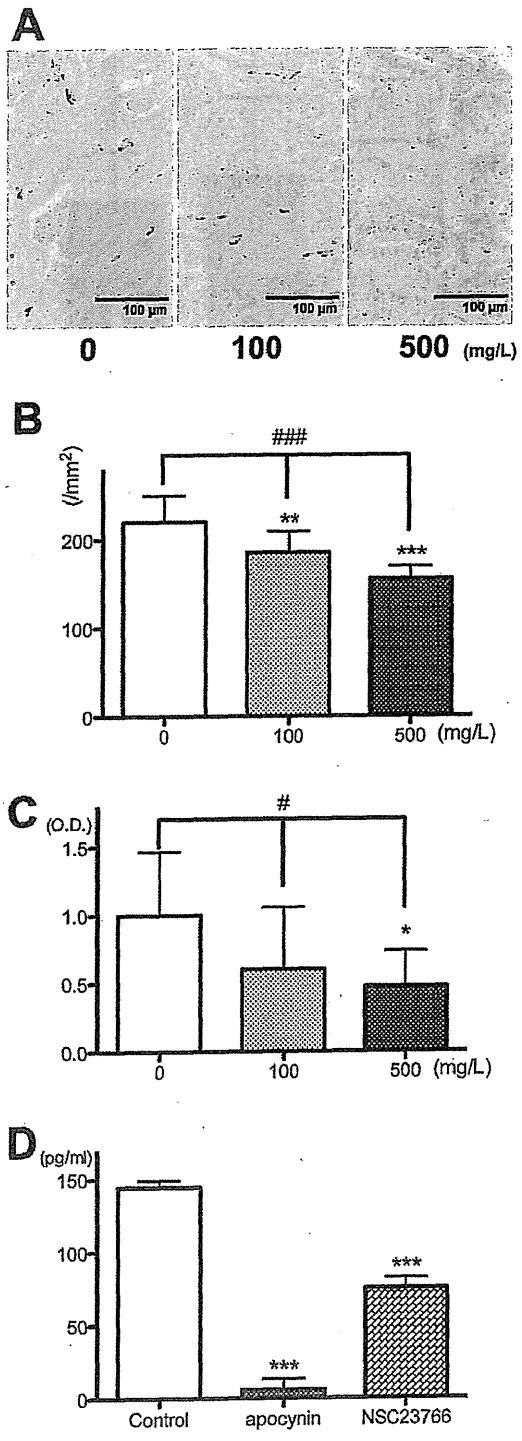

Fig. 4. Relationship between apocynin and angiogenesis. Vessels in the implanted tumors were detected with CD31 antibodies (A), and vessel number per unit area in the tumor are presented (B). VEGF expression in a tumor detected by immunostaining (C). VEGF secretion from PLS10 cells detected by ELISA in vitro (D). ### and #Spearman's rank correlation coefficient: rho = −0.78, $P < 0.001$ and rho = −0.45, $P < 0.05$. *, **, ***$P < 0.01$ and 0.001 compared to 0 mg/L or Control, respectively.

VEGF in tumors. Earlier reports indicated that ROS produced by NADPH oxidase stimulate diverse redox signaling pathways leading to angiogenic responses in endothelial cells and neovascularization in vivo (Ushio-Fukai et al., 2002; Ushio-Fukai, 2006). Therefore, apocynin may have a potential to inhibit tumor growth by blocking angiogenesis directly and indirectly in vivo.

Concerning mechanisms of anti-tumor effects by apocynin in prostate cancer, we detected reduction of NF-κB activation in PLS10 cells. NF-κB is known to be activated in tumor cells and induce cell proliferation, anti-apoptosis, angiogenesis, invasion and/or metastasis in various tumors including human prostate cancer (Prasad et al., 2010; Suh and Rabson, 2004). We found that apocynin inhibited VEGF secretion and cell proliferation via down-regulation of cyclin D1, which might be regulated by NF-κB activation in rat prostate cancer cell lines. Both apocynin and Rac1 inhibitor reduced phosphorylation of NF-κB in line with reports that Rac1 stimulates NF-κB activation in lung and prostate cancers (Sanlioglu et al., 2001; Fan et al., 2009). These data further suggest that the Rac1 pathway is important for prostate cancer development.

In conclusion, apocynin, an NADPH oxidase inhibitor, suppressed tumor growth of androgen-independent prostate cancer in vitro and in vivo. One possible mechanism of action is via Rac1 inactivation. In vivo, apocynin had the potential to inhibit tumor growth directly and indirectly via angiogenesis. Therefore, apocynin warrants further attention as a promising anti-tumor drug for androgen-independent prostate cancer.

5. Conflict of interest

The authors declare no conflict of interest.

Acknowledgements

This work was supported in part by grants from Ono Pharmaceutical Co., Ltd. and the Society for Promotion of Pathology in Nagoya, and the Research Foundation for Oriental Medicine.

References

Bedard K, Krause KH. The NOX family of ROS-generating NADPH oxidases: physiology and pathophysiology. Physiological Reviews 2007;87:245–313.
Bokoch GM, Diebold BA. Current molecular models for NADPH oxidase regulation by Rac GTPase. Blood 2002;100:2692–6.
Damber JE, Aus G. Prostate cancer. Lancet 2008;371:1710–21.
Fan S, Meng Q, Laterra JJ, Rosen EM. Role of Src signal transduction pathways in scatter factor-mediated cellular protection. Journal of Biological Chemistry 2009;284:7561–77.
Hordijk PL. Regulation of NADPH oxidases: the role of Rac proteins. Circulation Research 2006;98:453–62.
Jemal A, Bray F, Center MM, Ferlay J, Ward E, Forman D. Global cancer statistics. CA Cancer Journal for Clinicians 2011;61:69–90.
Khandrika L, Kumar B, Koul S, Maroni P, Koul HK. Oxidative stress in prostate cancer. Cancer Letters 2009;282:125–36.
Kobayashi T, Inoue T, Shimizu Y, Terada N, Maeno A, Kajita Y, Yamasaki T, Kamba T, Toda Y, Mikami Y, Yamada T, Kamoto T, Ogawa O, Nakamura E. Activation of Rac1 is closely related to androgen-independent cell proliferation of prostate cancer cells both in vitro and in vivo. Molecular Endocrinology 2010;24:722–34.
Kumar B, Koul S, Khandrika L, Meacham RB, Koul HK. Oxidative stress is inherent in prostate cancer cells and is required for aggressive phenotype. Cancer Research 2008;68:1777–85.
Lee YJ, Lee JH, Han HJ. Extracellular adenosine triphosphate protects oxidative stress-induced increase of p21(WAF1/Cip1) and p27(Kip1) expression in primary cultured renal proximal tubule cells: role of PI3K and Akt signaling. Journal of Cellular Physiology 2006;209:802–10.
Nakanishi H, Takeuchi S, Kato K, Shimizu S, Kobayashi K, Tatematsu M, Shirai T. Establishment and characterization of three androgen-independent, metastatic carcinoma cell lines from 3,2′-dimethyl-4-aminobiphenyl-induced prostatic tumors in F344 rats. Japanese Journal of Cancer Research 1996;87:1218–26.
Prasad S, Ravindran J, Aggarwal BB. NF-kappaB and cancer: how intimate is this relationship. Molecular and Cellular Biochemistry 2010;336:25–37.
Rosenkranz AR, Schmaldienst S, Stuhlmeier KM, Chen W, Knapp W, Zlabinger GJ. A microplate assay for the detection of oxidative products using 2′,7′-dichlorofluorescin-diacetate. Journal of Immunological Methods 1992;156:39–45.

Sanlioglu S, Luleci G, Thomas KW. Simultaneous inhibition of Rac1 and IKK pathways sensitizes lung cancer cells to TNFalpha-mediated apoptosis. Cancer Gene Therapy 2001;8:897–905.
Stefanska J, Pawliczak R. Apocynin: molecular aptitudes. Mediators of Inflammation 2008;2008:106507.
Stolk J, Hiltermann TJ, Dijkman JH, Verhoeven AJ. Characteristics of the inhibition of NADPH oxidase activation in neutrophils by apocynin, a methoxy-substituted catechol. American Journal of Respiratory Cell and Molecular Biology 1994;11:95–102.
Suh J, Rabson AB. NF-kappaB activation in human prostate cancer: important mediator or epiphenomenon? Journal of Cellular Biochemistry 2004;91:100–17.
Suzuki S, Arnold LL, Pennington KL, Kakiuchi-Kiyota S, Cohen SM. Effects of co-administration of dietary sodium arsenite and an NADPH oxidase inhibitor on the rat bladder epithelium. Toxicology 2009;261:41–6.
Ushio-Fukai M. Redox signaling in angiogenesis: role of NADPH oxidase. Cardiovascular Research 2006;71:226–35.
Ushio-Fukai M, Tang Y, Fukai T, Dikalov SI, Ma Y, Fujimoto M, Quinn MT, Pagano PJ, Johnson C, Alexander RW. Novel role of gp91(phox)-containing NAD(P)H oxidase in vascular endothelial growth factor-induced signaling and angiogenesis. Circulation Research 2002;91:1160–7.
Wu WS. The signaling mechanism of ROS in tumor progression. Cancer and Metastasis Reviews 2006;25:695–705.

IJC
International Journal of Cancer

2-Amino-1-methyl-6-phenylimidazo[4,5-b]pyridine (PhIP)-DNA adducts in benign prostate and subsequent risk for prostate cancer

Deliang Tang[1], Oleksandr N. Kryvenko[2], Yun Wang[3], Sheri Trudeau[3], Andrew Rundle[4], Satoru Takahashi[5], Tomoyuki Shirai[5] and Benjamin A. Rybicki[3]

[1] Department of Environmental Health Sciences, Columbia University, New York, NY
[2] Department of Pathology, Henry Ford Health System, Detroit, MI
[3] Department of Public Health Sciences, Henry Ford Health System,, Detroit, MI
[4] Department of Epidemiology, Columbia University, New York, NY
[5] Department of Pathology, Nagoya City University Medical School, Nagoya, Japan

Despite convincing evidence that 2-amino-1-methyl-6-phenylimidazo[4,5-b]pyridine (PhIP)—a heterocyclic amine generated by cooking meats at high temperatures—is carcinogenic in animal models, it remains unclear whether PhIP exposure leads to increased cancer risk in humans. PhIP-DNA adduct levels were measured in specimens from 534 prostate cancer case-control pairs nested within a historical cohort of men with histopathologically benign prostate specimens. We estimated the overall and race-stratified risk of subsequent prostate cancer associated with higher adduct levels. PhIP-DNA adduct levels in benign prostate were significantly higher in Whites than African Americans (0.274 optical density units (OD) ±0.059 *vs.* 0.256 OD ±0.054; $p<0.0001$). Prostate cancer risk for men in the highest quartile of PhIP-DNA adduct levels was modestly increased [odds ratio (OR) = 1.25; 95% confidence interval (CI) = 0.76–2.07]. In subset analyses, the highest risk estimates were observed in White patients diagnosed more than 4 years after cohort entry (OR = 2.74; 95% CI = 1.01–7.42) or under age 65 (OR = 2.80; 95% CI = 0.87–8.97). In Whites, cancer risk associated with high-grade prostatic intraepithelial neoplasia combined with elevated PhIP-DNA adduct levels (OR = 3.89; 95% CI = 1.56–9.73) was greater than risk associated with either factor alone. Overall, elevated levels of PhIP-DNA adducts do not significantly increase prostate cancer risk. However, our data show that White men have higher PhIP-DNA adduct levels in benign prostate tissue than African American men, and suggest that in certain subgroups of White men high PhIP-DNA adduct levels may predispose to an increased risk for prostate cancer.

2-Amino-1-methyl-6-phenylimidazo[4,5-*b*]pyridine (PhIP) is the most abundant heterocyclic amine (HCA) formed during the cooking of meat,[1] and a potential dietary risk factor for prostate and other cancers. A direct correlation between PhIP exposure, DNA adduct formation and other indicators of prostate carcinogenesis is supported by animal models and *in vitro* studies of human tissues. Rats fed a PhIP-laden diet for 52 weeks had PhIP-DNA adducts in all prostate lobes and subsequently developed prostate cancer[2]; PhIP exposure in rats is also associated with elevated mutation frequencies in prostate tissue[3] and increased prostate tumor incidence.[4] Mice administered PhIP showed positive staining for PhIP-DNA adducts in human prostate xenografts.[5] More recently, inflammation, atrophy of acini and prostatic intraepithelial neoplasia were observed in the prostate glands of a *CYP1A*-humanized mouse model, following a single oral dose of PhIP.[6]

Several *in vitro* studies of human prostate tissue incubated in PhIP-laden milieu have demonstrated detectable PhIP-DNA adducts in prostate cells.[7–9] While one study found a low prevalence of detectable PhIP-DNA adducts in prostate tissue using the ^{32}P-postlabeling method,[10] our own studies have demonstrated that PhIP-DNA adduct levels in prostate are related to dietary intake[11,12] and tumor grade.[13] *In vitro* experiments using the comet assay, and human prostate epithelial cells have shown that increased doses of PhIP result in increased DNA damage.[14] A study using a modified *in vitro* mutagen sensitivity assay, with activated PhIP (N-OH-PhIP) as the challenge mutagen and chromosomal aberrations as

Key words: dNA adducts, nested case–control study, immunohistochemistry, carcinogens, imidazoles, biopsy, needle

Abbreviations: BSA: bovine serum albumin; CI: confidence interval; HCA: heterocyclic amine; HGPIN: high-grade prostatic intraepithelial neoplasia; OD: optical density units; OR: odds ratio; PhIP: 2-amino-1-methyl-6-phenylimidazo[4,5-b]pyridine; PSA: prostate specific antigen; UGT: UDP-glucuronosyltransferases

Additional supporting information may be found in the online version of this article.

Grant sponsor: National Institutes of Health; **Grant number:** 5R01-ES011126

DOI: 10.1002/ijc.28092

History: Received 23 Nov 2012; Accepted 16 Jan 2013; Online 7 Feb 2013

Correspondence to: Benjamin A. Rybicki, PhD, One Ford Place 3E, Detroit, Michigan 48202, USA, Tel.: 313-874-6360, Fax: +313-874-6730, E-mail: brybick1@hfhs.org

What's new?

While exposure to high levels of PhIP (2-amino-1-methyl-6-phenylimidazo[4,5-b]pyridine)—a heterocyclic amine found in cooked meat—is associated with the development of prostate malignancies in animals, it is unclear whether this same risk exists in humans. Here, risk of prostate cancer in men was found to be increased only in the presence of both glandular inflammation and elevated levels of PhIP-DNA adducts, based on analysis of benign prostate specimens. However, certain subgroups of White males, who had higher PhIP-DNA adduct levels than African Americans, may be at greater risk for the disease. Given the putative role of inflammation in cancer, targeted prevention strategies in men with known high PhIP exposure levels may lead to beneficial health outcomes.

the endpoint, found that prostate cancer cases showed significantly higher numbers of breaks,[15] suggesting a greater susceptibility to PhIP-induced carcinogenesis in prostate cancer cases.

Despite the strong evidence for PhIP-induced prostate carcinogenesis from animal and *in vitro* studies, studies of dietary PhIP exposure and human prostate cancer risk are largely equivocal.[16–21] One limitation of these studies is their reliance on food frequency questionnaires to estimate PhIP exposure. While dietary intake data is informative, it is ultimately a poor measure of biologically effective dose, as it does not account for individual variation in PhIP metabolism or DNA repair capacity, which can influence DNA adduct formation.[11] Cellular and molecular changes are likely to be more relevant to disease outcome than measurement of PhIP in the diet. As such, the detection and quantification of PhIP-DNA adducts within the tissue of interest is an important step toward understanding the connection between exposure and cancer development. Case-control studies of PhIP-DNA adducts and cancer risk are limited to two studies, one of breast[22] and the other of pancreas,[23] both of which found elevated PhIP-DNA adducts in cancer patients. No studies have examined PhIP-DNA adducts levels in benign tissue and subsequent prostate cancer risk. Our own previous research on PhIP-DNA adduct levels was a cross-sectional study without a control group, using prostate tissue from cancer cases.[11–13]

In this study, we advance the molecular epidemiologic study of DNA adducts and cancer risk by measuring PhIP-DNA adduct levels in histopathologically normal tissue specimens taken from the target organ, and assess the relationship between adduct levels, pre-neoplastic histological markers, and subsequent cancer risk using a case-control study nested within a large historical cohort. In addition to testing whether adduct levels in histopathologically benign target tissue were associated with incident prostate cancer and tumor aggressiveness, we also explored race-specific cancer associations.

Methods

Study sample and medical record review

After obtaining approval from the Henry Ford Health System Institutional Review Board, we identified a historical cohort of 6,692 men with a benign prostate specimen collected by needle core biopsy or transurethral resection of the prostate (TURP) between January 1990 and December 2002. A nested case–control sample was drawn from this cohort based on eligibility criteria that included a recorded prostate specific antigen (PSA) level within a year of cohort entry and no history of a previous prostate cancer diagnosis. "Date of cohort entry" was defined as the date that the initial benign prostate specimen was acquired; "date of case diagnosis" was the date of first cancer-positive tissue specimen or the date a clinician first reported a clinical diagnosis of prostate cancer. Patients diagnosed with prostate cancer less than one year from date of cohort entry were ineligible for the study. We identified 808 potentially eligible cases diagnosed with prostate cancer prior to July 2007.

Incidence density sampling was used to select controls without replacement from all cohort members at risk at the time of case occurrence. Controls were randomly selected from among those cohort members who were free of prostate cancer at a follow-up duration greater than or equal to the time between cohort entry and diagnosis dates of the matched cases, with the end of follow-up denoted as the "reference date" for controls. Matching criteria included age at entry into cohort (±2 years), date of entry into cohort (±2 years), race (African American or White) and type of specimen (biopsy or TURP). We were able to match 802 of 808 potentially eligible cases. Further review reduced the final analytic sample to 574 case-control pairs,[24] of which we were able to analyze the PhIP-DNA adduct levels in 534 pairs; the remaining 40 pairs were excluded due to absence of sufficient numbers of epithelial cells in the tissue specimen.

Smoking status, and clinical, demographic, and co-morbidity data were abstracted from patients' medical records from 5 years before the date of cohort entry through the date of diagnosis (for prostate cancer cases) or reference date (for controls). All medical data used in study analyses are based on the date of cohort entry unless otherwise noted.

Immunohistochemistry

Consecutive sections (5-micron thick) were cut from each formalin-fixed, paraffin-embedded prostate specimen; one slide was used for PhIP-DNA adduct detection as described below and the other was hematoxylin and eosin (H&E) stained and examined by a single genitourinary pathologist

(O.N.K.) blinded to disease progression. The pathology examination included evaluation of the specimen for the presence of cancer, high-grade prostatic intraepithelial neoplasia (HGPIN), atrophy, and inflammation.[24]

Paraffin-embedded sections were heated to 50°C for 1 hr, deparaffinized in xylene, and rehydrated in serial alcohol. After treatment with RNase and Proteinase K, the sections were blocked using 3% bovine serum albumin (BSA) and normal goat serum. Sections were incubated in a humid 4°C chamber overnight with a 1:500 dilution of the primary anti-PhIP-DNA adduct polyclonal antibody[2,25]; then incubated at room temperature for 30 min with a 1:200 dilution of the biotinylated secondary antibody. Specimens were bathed in 0.3% hydrogen peroxide in methanol for 20 min to block endogenous peroxidase activity.

The PhIP-DNA polyclonal antibody recognizes DNA adducts at the C8 position of deoxyguanosine as the epitope. The PhIP-modified DNA antigen contains N^2-(2′-deoxyguanosin-8-yl)-PhIP,[25] which is recognized as the major adduct formed between PhIP and DNA.[26] Specificity of the PhIP-DNA adduct antibody was evaluated in liver tissue of rats separately exposed for 6 weeks to HCAs as follows: 3-amino-1,4-dimethyl-5H-pyrido[4,3-b]indole (Trp-P-1, 150ppm); 2-aminodipyrido[1,2-a:3′,2′-d]imidazole (Glu-P-2, 500ppm); 2-amino-3-methylimidazo[4,5-f]quinoline (MeIQ, 300ppm); or 2-amino-3,8-dimethylimidazo[4,5-f]quinoxaline (MeIQx, 400ppm). Presence of DNA adducts was confirmed by the ^{32}P-postlabeling method.[27] No cross-reactivity with any HCA-DNA adducts was found (S. Takahashi, unpublished data).

The antibody complex was detected using an avidin-biotin-peroxidase complex solution and visualized using 3,3′-diaminobenzidine chromogen (Zymed Laboratories, San Francisco, CA). A negative control was included in each experiment by omitting the primary antibody. A cytospin sample of MCF-7 cells without PhIP treatment was included in each batch of staining. Staining was measured by absorbance image analysis using the Cell Analysis System 200 (Becton Dickinson, San Jose, CA). Absorbance of light at a wavelength of 500 nmol/L was measured in optical density units (OD). Previous calibration studies using N-hydroxy-PhIP-treated MCF-7 cells have demonstrated optical density sensitivity to N-hydroxy-PhIP adducts ranging from 1 to 100 μM with a detection limit of about $1/10^7$ for PhIP-DNA adducts.[22] For each specimen, a technician scored 50 epithelial cells (five fields, ten cells per field) selected to be representative, in terms of intensity, of the cells in the field.

Statistical analysis

Conditional logistic regression analyses were used to estimate both unadjusted and adjusted odds ratios (ORs) for prostate cancer incidence during follow-up. Individual matching controlled for age, race, and specimen type (biopsy or TURP). Analyses were performed using adduct levels expressed as both continuous and categorical variables; for the latter, adduct distribution was segmented among control subjects into referent categories. Potential confounders were identified by first testing whether the variable was associated with case status or adduct levels; associated variables were then tested in multivariable models to determine whether their inclusion changed the effect estimate by 10% or more. Comparisons between stratified models were assessed using conditional logistic regression with interaction terms.

Results

Study sample and PhIP-DNA adduct levels

In the analytic sample of 534 pairs, cases were an average of 65.4 years old at cohort entry and 40% were African American (supporting information Table 1). The 40 pairs with unanalyzable adduct data were significantly older (2.5 years, $p = 0.05$), had 0.8 more PSA tests between cohort entry and diagnosis ($p = 0.05$), and entered the cohort earlier (median 21 months, $p = 0.03$) than those that were analyzed. In the full sample, median time to diagnosis was 1–4 years after cohort entry, with the remaining cases diagnosed 4–15 years after cohort entry. Cases had significantly higher PSA levels at time of cohort entry (7.7 ± 7.3 ng/mL *vs.* 5.6 ± 5.3 ng/mL; $p < 0.0001$) and averaged two more PSA tests between cohort entry and diagnosis. The majority of cases (52.6%) had Stage 2 tumors; 29% of cases had advanced tumor grade defined as either Gleason score 8 and above or Gleason score 7 with a primary Grade 4. Mean PhIP-DNA adduct levels were slightly elevated in cases compared with controls, but the difference was not statistically significant (0.263 OD $\pm$ 0.058 *vs.* 0.260 OD $\pm$ 0.045; $p = 0.32$).

Factors associated with PhIP-DNA adduct levels

Given the known association between race and differences in both exposure to and metabolism of PhIP,[13,28–30] we tested whether PhIP-DNA adduct levels varied by race. Mean adduct levels were significantly higher in Whites than African Americans (0.276 ± 0.059 *vs.* 0.257 ± 0.053 OD; $p < 0.0001$) and followed a normal distribution in both racial groups (supporting information Figure 1).

To better understand how the histological characteristics of prostate tissue might affect PhIP-DNA adduct levels, we estimated the mean adduct levels by histological variables that were previously described in this sample (Table 1).[24] In White patients with partial atrophy, we observed significantly higher levels of PhIP-DNA adducts than in those without partial atrophy (0.285 ± 0.060 *vs.* 0.272 ± 0.059 OD; $p = 0.01$); the same trend in adduct levels was observed in the benign prostate specimens derived from African American patients, but differences between groups were smaller. Conversely, in African Americans with glandular inflammation, adduct levels were significantly higher than in those without glandular inflammation (0.239 ± 0.057 *vs.* 0.260 ± 0.051 OD; $p = 0.005$), and a similar, but less significant inverse association was observed in Whites. In an effort to further tease apart the association of atrophy with adduct

Table 1. Mean PhIP-DNA adduct levels in optical density units stratified by race and histological variables

	Mean optical density units ± standard deviation								
	Whole sample			African Americans			Whites		
Variable	Present	Absent	*p* value	Present	Absent	*p* value	Present	Absent	*p* value
HGPIN	0.272 ± .054 ($n = 74$)	0.268 ± .058 ($n = 838$)	0.60	0.253 ± .048 ($n = 31$)	0.257 ± .053 ($n = 323$)	0.69	0.285 ± .055 ($n = 43$)	0.275 ± .060 ($n = 515$)	0.28
Atrophy	0.269 ± .058 ($n = 736$)	0.266 ± .058 ($n = 176$)	0.45	0.257 ± .054 ($n = 285$)	0.256 ± .049 ($n = 69$)	0.86	0.277 ± .059 ($n = 451$)	0.272 ± .063 ($n = 107$)	0.43
Simple atrophy	0.269 ± .057 ($n = 656$)	0.269 ± .060 ($n = 256$)	0.95	0.256 ± .053 ($n = 253$)	0.260 ± .051 ($n = 101$)	0.51	0.277 ± .057 ($n = 403$)	0.274 ± .065 ($n = 155$)	0.62
Post-atrophic hyperplasia	0.282 ± .050 ($n = 18$)	0.268 ± .058 ($n = 894$)	0.34	0.308 ± .021 ($n = 3$)	0.257 ± .053 ($n = 351$)	0.09	0.276 ± .053 ($n = 15$)	0.279 ± .060 ($n = 543$)	0.99
Simple atrophy—cyst formation	0.264 ± .061 ($n = 175$)	0.270 ± .057 ($n = 737$)	0.28	0.258 ± .064 ($n = 54$)	0.257 ± .050 ($n = 300$)	0.88	0.267 ± .060 ($n = 121$)	0.279 ± .059 ($n = 437$)	0.07
Partial atrophy	0.277 ± .059 ($n = 267$)	0.265 ± .057 ($n = 645$)	0.006	0.260 ± .051 ($n = 91$)	0.256 ± .053 ($n = 263$)	0.45	0.285 ± .060 ($n = 176$)	0.272 ± .059 ($n = 382$)	0.01
Inflammation	0.267 ± .056 ($n = 551$)	0.272 ± .059 ($n = 361$)	0.18	0.254 ± .053 ($n = 219$)	0.261 ± .051 ($n = 135$)	0.24	0.275 ± .057 ($n = 332$)	0.278 ± .063 ($n = 226$)	0.48
Glandular inflammation	0.259 ± .059 ($n = 169$)	0.271 ± .057 ($n = 743$)	0.02	0.239 ± .057 ($n = 56$)	0.260 ± .051 ($n = 298$)	0.005	0.270 ± .058 ($n = 113$)	0.278 ± .060 ($n = 445$)	0.18
Periglandular inflammation	0.264 ± .058 ($n = 364$)	0.272 ± .057 ($n = 548$)	0.04	0.251 ± .055 ($n = 148$)	0.262 ± .051 ($n = 206$)	0.05	0.273 ± .058 ($n = 216$)	0.278 ± .060 ($n = 342$)	0.31
Stromal inflammation	0.266 ± .056 ($n = 430$)	0.271 ± .059 ($n = 482$)	0.19	0.254 ± .053 ($n = 171$)	0.259 ± .052 ($n = 183$)	0.39	0.274 ± .056 ($n = 259$)	0.278 ± .063 ($n = 299$)	0.37

Table 2. Association of PhIP-DNA Adduct Levels with Prostate Cancer

Sample	OR[1]	95% CI	*p* value
PhIP-DNA adduct Level			
Whole sample ($n = 534$ case–control pairs)			
2nd Quartile	1.20	0.83–1.72	0.34
3rd Quartile	1.29	0.87–1.92	0.20
4th Quartile	1.25	0.76–2.07	0.38
Trend test			0.36
High PhIP level[2]	1.16	0.84–1.59	0.37
African Americans ($n = 213$ case–control pairs)			
2nd Quartile	1.32	0.75–2.32	0.33
3rd Quartile	0.96	0.49–1.86	0.90
4th Quartile	0.73	0.32–1.63	0.44
Trend test			0.35
High PhIP level[1]	0.76	0.44–1.32	0.33
Whites ($n = 321$ case–control pairs)			
2nd Quartile	1.12	0.69–1.81	0.65
3rd Quartile	1.48	0.90–2.44	0.13
4th Quartile	1.73	0.89–2.34	0.10
Trend Test			0.07
High PhIP level[2]	1.44	0.97–2.14	0.07

[1]All risk estimates use lowest level as referent group.
[2]Above median level in controls.

levels, we modeled PhIP-DNA adduct levels with covariates for both simple and partial atrophy adjusting for race and glandular inflammation. The least squares mean estimates of PAH-DNA adduct levels for the four possible combinations of simple and partial atrophy are shown in Figure 1. In cases, PhIP-DNA adduct levels were lowest when no atrophy was present, highest when only partial atrophy was present, and intermediate when simple atrophy was present (irrespective of whether partial atrophy was also present). In controls, there was no association between PhIP-DNA adduct levels and atrophy status; controls had higher levels of PhIP-DNA adducts than cases when no atrophy was observed, but much lower levels than cases when only partial atrophy was noted in the specimen. This same general pattern was observed when the data were stratified by race.

Prostate cancer risk associated with higher levels of PhIP-DNA adducts

While mean PhIP-DNA adduct levels did not differ significantly between cases and controls, previous studies have shown that the effect of DNA adducts on cancer-related outcomes tends to be non-linear.[31,32] Therefore, to determine whether prostate cancer risk was associated with elevated adduct levels, we tested two models, one in which adduct levels were categorized into quartiles, and another in which levels were dichotomized above and below the median (Table 2). Due to the differences of adduct levels by race, models for both the full sample as well as race-stratified models were tested. For the full sample, quartile risk estimates did not reach statistical significance nor was the trend statistically significant ($p = 0.36$); similarly, the OR for adduct levels greater than the median was also non-significant. When the sample was stratified by race, increased risk associated with elevated PhIP-DNA adduct levels trended upward in Whites: 12% for the 2nd quartile, 48% for the 3rd quartile, and 73% for the 4th quartile, but none were statistically significant, nor was the trend statistically significant ($p = 0.07$). Models adjusting for inflammation, atrophy, and number of PSA tests were also tested, but changes in risk estimates were nominal (data not shown).

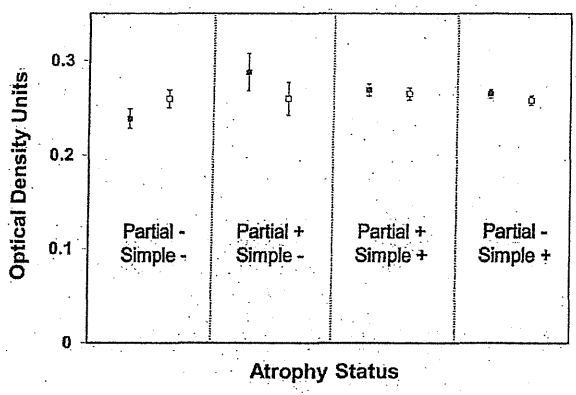

Figure 1. Least squares means estimates of PhIP-DNA adduct levels by case (shaded square)/control (open square) status and type of atrophy in the benign sample.

Table 3 reports risk estimates stratified by selected matching factors (including race) and tumor grade (for cases). In the full sample, little evidence for heterogeneity of high PhIP-DNA adduct levels by strata exists. In the White subsample—where elevated PhIP-DNA adduct levels had suggestive associations with prostate cancer risk—ORs were greater for cases with high tumor grade, longer follow-up, later cohort entry, and younger age at diagnosis. In White cases diagnosed before age 65, the risk of prostate cancer was elevated 70–80% in the 2nd and 3rd quartiles, and 180% in the 4th quartile, but neither risk estimates nor the linear trend test reached statistical significance.

The other stratum with markedly higher risk estimates was White cases diagnosed 4 years or more after cohort entry, where risk of prostate cancer was unchanged for the 2nd quartile, but increased 60% for the 3rd quartile and 174% for the 4th quartile. The risk estimate in the 4th quartile was marginally statistically significant [OR = 2.74; 95% confidence interval (CI) = 1.01–7.42] and the linear trend of risk estimates across quartiles was also statistically significant ($p = 0.03$). To further investigate whether this suggested a temporal relationship between adduct levels and prostate cancer, we analyzed the association between adduct quartile and

Table 3. Association of PhIP-DNA adduct levels with prostate cancer, stratified by matching factors and case characteristics

Sample	Whole sample			African Americans			Whites		
PhIP Level	OR[1]	95% CI	*p* value	OR	95% CI	*p* value	OR	95% CI	*p* value
Low tumor grade	(*n* = 367 case–control pairs)			(*n* = 137 case–control pairs)			(*n* = 230 case–control pairs)		
2nd Quartile	1.40	0.84–2.31	0.19	1.94	0.83–4.55	0.13	1.17	0.62–2.19	0.63
3rd Quartile	1.37	0.81–2.33	0.25	1.42	0.53–3.85	0.49	1.30	0.69–2.46	0.41
4th Quartile	1.29	0.65–2.54	0.47	1.09	0.30–4.01	0.90	1.36	0.61–3.04	0.46
Trend test			0.51			0.98			0.43
High tumor grade	(*n* = 138 case–control pairs)			(*n* = 56 case–control pairs)			(*n* = 82 case–control pairs)		
2nd Quartile	0.92	0.45–1.86	0.81	1.14	0.38–3.44	0.82	0.87	0.33–2.28	0.77
3rd Quartile	1.57	0.68–3.65	0.29	0.94	0.22–4.08	0.93	2.04	0.69–6.07	0.20
4th Quartile	1.03	0.31–3.39	0.97	0.45	0.07–2.96	0.41	1.84	0.34–10.00	0.48
Trend test		0.76			0.43			0.33	
1–4 years of Follow-up	(*n* = 266 case–control pairs)			(*n* = 103 case–control pairs)			(*n* = 163 case–control pairs)		
2nd Quartile	1.63	0.91–2.92	0.10	1.83	0.76–4.44	0.18	1.48	0.68–3.24	0.32
3rd Quartile	1.46	0.75–2.84	0.27	0.99	0.31–3.16	0.99	1.68	0.74–3.84	0.22
4th Quartile	1.15	0.49–2.69	0.74	0.95	0.23–4.02	0.95	1.23	0.42–3.55	0.71
Trend test			0.82			0.75			0.67
4–15 years of follow-up	(*n* = 267 case–control pairs)			(*n* = 110 case–control pairs)			(*n* = 157 case–control pairs)		
2nd Quartile	0.90	0.51–1.58	0.72	0.82	0.32–2.11	0.67	0.99	0.48–2.05	0.99
3rd Quartile	1.34	0.75–2.37	0.32	0.90	0.32–2.55	0.84	1.60	0.78–3.27	0.20
4th Quartile	1.46	0.70–3.03	0.31	0.62	0.17–2.18	0.45	2.74	1.01–7.42	0.05
Trend test			0.21			0.53			0.03
Early cohort entry	(*n* = 263 case–control pairs)			(*n* = 88 case–control pairs)			(*n* = 175 case–control pairs)		
2nd Quartile	1.28	0.69–2.40	0.44	2.46	0.69–8.76	0.17	1.02	0.49–2.12	0.96
3rd Quartile	1.28	0.68–2.40	0.44	1.92	0.56–6.53	0.30	1.09	0.52–2.29	0.83
4th Quartile	1.73	0.78–3.86	0.18	2.76	0.60–12.75	0.19	1.42	0.54–3.72	0.48
Trend test			0.21			0.27			0.47
Late cohort entry	(*n* = 270 case–control pairs)			(*n* = 125 case–control pairs)			(*n* = 145 case–control pairs)		
2nd Quartile	1.10	0.67–1.84	0.69	1.00	0.48–2.10	1.00	1.14	0.55–2.36	0.72
3rd Quartile	1.40	0.76–2.57	0.28	0.60	0.20–1.77	0.35	2.18	0.99–4.78	0.05
4th Quartile	0.98	0.46–2.13	0.97	0.29	0.08–1.08	0.06	2.14	0.73–6.24	0.16
Trend test			0.89			0.06			0.09
Age <65	(*n* = 274 case–control pairs)			(*n* = 110 case–control pairs)			(*n* = 164 case–control pairs)		
2nd Quartile	1.30	0.72–2.35	0.39	0.92	0.38–2.24	0.85	1.79	0.79–4.09	0.16
3rd Quartile	1.35	0.72–2.53	0.35	0.95	0.35–2.60	0.92	1.71	0.74–3.95	0.21
4th Quartile	1.08	0.47–2.47	0.85	0.38	0.10–1.42	0.15	2.80	0.87–8.97	0.08
Trend test			0.83			0.18			0.09
Age 65+	(*n* = 259 case–control pairs)			(*n* = 103 case–control pairs)			(*n* = 156 case–control pairs)		
2nd Quartile	1.10	0.64–1.89	0.72	1.71	0.65–4.50	0.27	0.82	0.41–1.62	0.56
3rd Quartile	1.45	0.79–2.67	0.23	1.02	0.29–3.60	0.97	1.55	0.76–3.16	0.22
4th Quartile	1.54	0.72–3.29	0.26	1.52	0.33–7.03	0.59	1.46	0.57–3.45	0.47
Trend test			0.23			0.78			0.28

[1]*All risk estimates use lowest quartile as referent group.*

Table 4. Effect modification of PhIP-DNA adduct level[1] associations with prostate cancer

	Whole sample ($n = 534$ case–control pairs)			African Americans ($n = 213$ case–control pairs)			Whites ($n = 321$ case–control pairs)		
Effect Modifier	**OR**	**95% CI**	***p* value**	**OR**	**95% CI**	***p* value**	**OR**	**95% CI**	***p* value**
PSA at cohort entry									
PSA < 4 ng mL/Low PhIP	1			1			1		
PSA < 4 ng mL/High PhIP	1.35	0.79–2.32	0.27	0.89	0.35–2.27	0.81	1.63	0.84–3.18	0.15
PSA ≥ 4 ng mL/Low PhIP	3.39	2.14–5.36	<0.0001	3.73	1.83–7.62	0.0003	3.08	1.69–5.63	0.0002
PSA ≥ 4 ng mL/High PhIP	3.21	2.00–5.15	<0.0001	2.37	1.08–5.19	0.03	3.62	1.99–6.58	<0.0001
PSA ≥ 4 ng mL × High PhIP interaction	0.70	0.39–1.27	0.24	0.71	0.26–1.93	0.51	0.72	0.34–1.52	0.39
Glandular inflammation									
No Inflammation/Low PhIP	1			1			1		
No Inflammation/High PhIP	1.06	0.75–1.48	0.75	0.70	0.40–1.25	0.23	1.29	0.84–1.96	0.25
Inflammation/Low PhIP	0.78	0.48–1.27	0.32	1.01	0.49–2.07	0.98	0.64	0.32–1.26	0.20
Inflammation/High PhIP	1.54	0.91–2.61	0.11	1.56	0.54–4.52	0.42	1.61	0.87–2.99	0.13
Inflammation × High PhIP interaction	1.87	0.95–3.68	0.07	2.19	0.65–7.43	0.21	1.97	0.83–4.69	0.13
HGPIN									
No HGPIN/Low PhIP	1			1			1		
No HGPIN/High PhIP	1.16	0.84–1.61	0.37	0.82	0.47–1.44	0.48	1.38	0.92–2.07	0.12
HGPIN/Low PhIP	2.16	1.07–4.37	0.03	2.88	1.04–7.98	0.04	1.52	0.55–4.16	0.42
HGPIN/High PhIP	2.25	1.12–4.51	0.02	0.79	0.24–2.59	0.69	3.89	1.56–9.73	0.004
HGPIN × High PhIP interaction	0.90	0.35–2.28	0.82	0.33	0.08–1.46	0.15	1.86	0.50–6.88	0.35
Partial Atrophy									
No atrophy/Low PhIP	1			1			1		
No atrophy/High PhIP	1.23	0.87–1.74	0.25	0.85	0.47–1.53	0.58	1.48	0.95–2.30	0.08
Atrophy/Low PhIP	0.98	0.66–1.46	0.92	1.12	0.62–2.02	0.72	0.89	0.51–1.54	0.67
Atrophy/High PhIP	1.00	0.66–1.74	1.00	0.59	0.27–1.28	0.18	1.25	0.76–2.08	0.38
Atrophy × High PhIP interaction	0.83	0.49–1.41	0.49	0.63	0.26–1.52	0.30	0.95	0.48–1.89	0.89

[1]High PhIP was considered above median level in controls.

time to diagnosis among White cases (supporting information Figure 2). While cases with elevated adduct levels were diagnosed more rapidly within 2–3 years of follow-up, the greatest difference in risk between the lowest and highest quartiles was observed 5–7 years after cohort entry. Overall, the four quartile curves for time to diagnosis were significantly different (log rank p-value = 0.05).

We next tested whether known clinical or histological prostate cancer risk factors modified the relationship between elevated PhIP-DNA adduct levels and prostate cancer (Table 4). Overall, no factors significantly modified the risk associated with elevated adduct levels and prostate cancer, although some interesting trends emerged. Partial atrophy and glandular inflammation were both associated with PhIP-DNA adducts in this study population in a race-specific manner, but neither modified the risk of prostate cancer associated with high adduct levels. Glandular inflammation had the highest interaction OR (OR = 2.19 in African Americans; 1.97 in Whites), and although neither OR was statistically significant, it appeared that elevated PhIP-DNA adduct levels increased risk for prostate cancer only in the presence of glandular inflammation. HGPIN was associated with prostate cancer in this study population,[24] and it modestly enhanced the association between elevated adduct levels and prostate cancer in Whites. In the absence of HGPIN, elevated PhIP-DNA adducts increased the risk for prostate cancer by 38%, but in the presence of both HGPIN and high PhIP-DNA adducts level, the risk increased almost four-fold (OR = 3.89; CI = 1.56–9.73). This is in contrast to what was observed in African Americans where the combination of HGPIN and elevated PhIP-DNA adduct levels actually decreased prostate cancer risk.

Discussion

We report for the first time a prospective analysis of PhIP-DNA adduct levels—a marker of biologically effective exposure to PhIP—measured in histopathologically benign tissue, and subsequent cancer risk for the same organ. Prior prospective studies of adduct levels and cancer risk have used surrogate tissues, such as white blood cells, but the correlation between adduct levels in these surrogate tissues *versus* the target organ is unclear.[33,34] Here we find that higher levels of PhIP-DNA adducts in benign prostate specimens were associated with a modestly increased risk for prostate cancer in White men. When the analysis was restricted to White cases diagnosed more than 4 years after tissue collection, however, patients with the highest PhIP-DNA adduct levels had almost three-fold increased risk of prostate cancer. In African Americans, we did not detect any observable increased risk associated with high PhIP-DNA adduct levels, in either the full sample or subgroups.

Until now, the question of whether PhIP increases risk for prostate cancer has largely been addressed using estimated dietary consumption of PhIP.[35] The first such effort found no increased risk of prostate cancer with increasing PhIP consumption.[36] A subsequent prospective study found a modest 22% increased prostate cancer risk for the highest PhIP consumption, with a statistically significant trend.[21] Since that study, multiple cohort[17,18,20] and case-control[16,19] questionnaire-based studies have been performed, collectively providing equivocal results concerning dietary PhIP consumption and prostate cancer risk. Given the high potential for measurement error using questionnaire data, biomarker studies are needed to address the potential carcinogenicity of this compound.

Despite availability of an anti-PhIP-DNA adduct antibody for immunohistochemistry studies,[12,22,25], only two case-control studies of cancer have employed this method previously; both finding higher PhIP-DNA adduct levels in benign tissue of the cancer-affected organ of cases compared with the corresponding tissue of controls.[22,23] Adduct levels were four times more likely to be high in benign tissue of breast cancer cases than controls[22] and 3.5 times more likely to be high in benign tissue of pancreatic cancer cases than controls.[23] To date, ours is the first such study to be performed in human prostate and the only study of PhIP-DNA adduct levels in pre-disease tissue.

Our previous study of men with prostate cancer found no racial differences in PhIP adduct levels in prostate tissue,[13] but in this study, we found that Whites had significantly higher levels of PhIP adducts in benign prostate than African Americans. Dietary data strongly suggest African Americans have higher exposure to PhIP through food preparation methods that differ by race[28] and African Americans have been shown to excrete more PhIP in urine.[30] Both activation and detoxification of PhIP play a role in adduct formation. African American men have slightly higher activity levels of the PhIP-metabolizing enzyme SULT1A1 than Whites.[29] However, both African Americans and Whites show an association between prostate cancer risk, SULT1A1 levels, and the Arg213His functional polymorphism in the *SULT1A1* gene.[29] African Americans also have higher enzymatic activity levels of CYP1A2 and N-acetyltransferase,[37] two enzymes important in the O-acetylation and N-oxidation of PhIP, respectively. PhIP and its carcinogenic metabolite N-hydroxy-PhIP (N-OH-PhIP) are extensively conjugated by UDP-glucuronosyltransferases (UGTs),[9] and UGT1A1 is the predominant UGT involved in PhIP metabolism[38]; notably, the most prevalent *UGT1A1* genotype in African Americans is associated with a lower capacity to detoxify PhIP.[39] While PhIP detoxification by UGT1A1 appears to be less efficient in African Americans, a study of *UGT1A1* genetic variation and colon cancer risk found an elevated risk associated with intermediate- to low-activity *UGT1A1* genotypes in Whites but not in African Americans.[40] This is consistent with our recent study that found non-specific genetic variation related to African ancestry to be a stronger predictor of PhIP-DNA adduct levels in prostate tissue than genetic variation in either *UGT1A1* or *SULT1A1*.[11] While the literature reviewed above would suggest that African Americans should have higher PhIP-DNA adduct levels and subsequently a greater risk of cancer associated with this marker than Whites, our results suggest the opposite. Clearly the carcinogenic potential of PhIP in human prostate is more complex than the sum of what is currently known about race-specific dietary exposure and genetic variation in PhIP metabolism.[41,42]

Our findings may be better understood by considering the histological cofactors we found to be associated with adduct levels. Inflammation and atrophy are hypothesized to be precursors of prostate cancer.[43,44] Inflammatory cytokines are known to suppress the activity of CYP1A enzymes[45] which is expressed in human prostate tumor and normal cells[46,47]; experimental evidence has shown that human prostate cells can activate PhIP and incur subsequent downstream effects such as DNA adduct formation and damage.[8,48] We found that adduct levels were higher when partial atrophy was present, and that PhIP-DNA adducts and HGPIN may act synergistically to increase prostate cancer risk in White men. In both races, adduct levels were highest in cases with partial but no simple atrophy and prostate cancer risk was increased only in the presence of both high PhIP-DNA adduct levels and glandular inflammation. Based on these findings we propose the model described in Figure 2 as to how PhIP might increase prostate cancer risk in humans. This model assumes variation in inherited susceptibility to metabolize PhIP and other dietary cofactors. The state of the inflammatory environment within the PhIP-exposed prostate is potentially related to both the amount of PhIP-DNA adducts created and prostate cancer risk.

Our study was observational, and while the duration of at-risk follow-up was equal for cases and controls, cohort members differed in their medical follow-up and screening behavior. Cases had significantly more PSA tests between cohort entry and diagnosis than controls, and the frequency of PSA tests in our study sample was greater than current

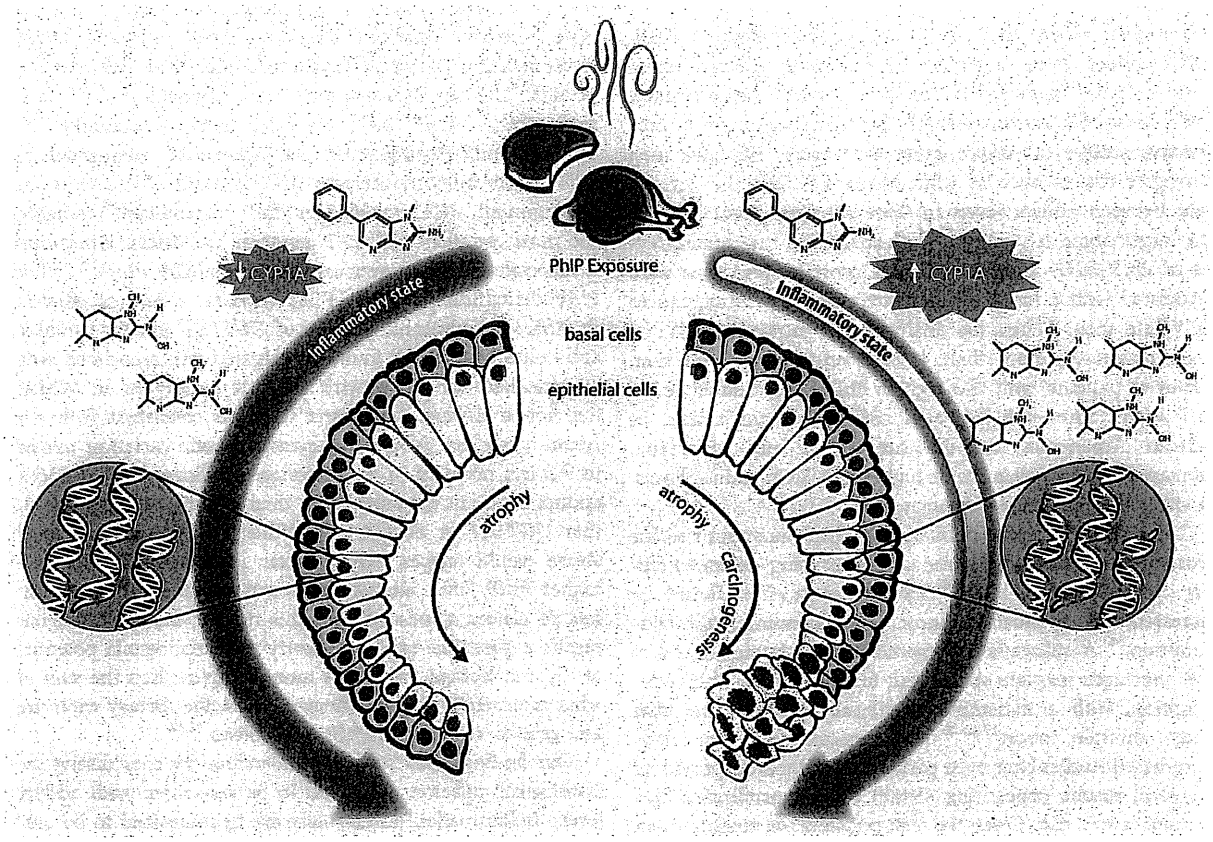

Figure 2. Proposed model of PhIP metabolism and DNA adduct formation in human prostate in relation to inflammation, atrophy and cancer risk. Depending on inherited susceptibility and level of dietary intake, PhIP exposure elicits a variable inflammatory response. A strong response (left side of figure) may dampen the expression of CYP1A enzymes, leading to accumulation of fewer active PhIP metabolites (N_2-hydroxy-PhIP), and subsequently lower levels of DNA adducts; a strong inflammatory response would also accelerate atrophy of prostate glandular cells, but not necessarily lead to carcinogenesis. Alternatively, a weak inflammatory response to PhIP exposure (right side of figure) may result in higher CYP1A activity levels, generation of more active PhIP metabolites, and subsequently higher levels of DNA adducts, but the progression of cellular atrophy would not be as rapid. A late elevated inflammatory response coupled with high levels of DNA adducts could incite prostate carcinogenesis. [Color figure can be viewed in the online issue, which is available at wileyonlinelibrary.com]

screening recommendations, even in controls. However, there is no *a priori* reason why screening behavior should differ by adduct levels and, indeed, adjustment for number of PSA tests during follow-up did not substantively change our results. While we were able to analyze 93% of eligible pairs, included pairs were slightly over-represented by younger cases and newer tissue samples, which tended to show stronger associations between PhIP-DNA adduct levels and prostate cancer risk in Whites. Based on the age range of our cohort and the high prevalence of undiagnosed prostate cancer in older men,[49] some men in our cohort likely had synchronous prostate cancer that was missed on initial biopsy. One would expect these cohort members misclassified as "disease-free" to be diagnosed sooner[50] and bias risk estimates toward the null. Hence risk estimates in men with longer follow-up may be less biased—suggesting that the greater prostate cancer risk associated with high PhIP-DNA adduct levels we observed in White men with four or more years of follow-up is closer to the true risk estimate.

In using a semi-quantitative immunohistochemical assay to measure PhIP-DNA adduct levels, our results are subject to several limitations. The specificity of the antibody we used to detect PhIP-DNA adducts has not been validated against the full range of possible mutagenic HCAs generated in well-done meats; most notably, we were unable to test whether the antibody could distinguish between PhIP-DNA and 2-amino-3,4,8-dimethylimidazo[4,5-f]quinoxaline (DiMeIQx)-DNA adducts. Despite this, we believe our results remain valid for several reasons. Although several studies using food preparation questionnaire data suggest an increased prostate cancer risk associated with DiMeIQx intake,[16,17] to our knowledge, laboratory studies have not detected DiMeIQx-DNA adducts in prostate tissue. Furthermore, we have previously reported a dose–response relationship between grilled red meat intake

and prostate tissue levels of the same PhIP-DNA adduct antibody used in this study[12] even though DiMeIQx is present only in trace amounts in beef products.[53] Levels of PhIP in other cooked meats are also generally an order of magnitude greater than levels of DiMeIQx; as a result, DiMeIQx intake is unlikely to confound PhIP exposure measurements.[51,52] More sensitive methods of PhIP-DNA adduct detection have been attempted in only two human studies; neither studied prostate tissue, and the percentage of "undetectable" samples varied significantly between them.[54,55] Based on previously reported calibration studies of the PhIP-DNA adduct antibody,[22] the absorbency measure we used can detect roughly a 100-fold range difference in PhIP-DNA adduct concentration, with a lower limit of detection around $1/10^7$ nucleotides. While such a level might seem unrealistic in humans, a study using mass spectrometry detected PhIP-DNA adducts in lymphocytes at a level of 3×10^8 nucleotides.[55] Finally, because our study categorized the adduct data, it can be assumed that specimens with adduct levels undetectable by more sensitive methods would be in the lowest category, and serve as the reference group in statistical analyses. In addition, analysis of adduct data as categorical variables defined around the median ensured that measurement inaccuracies at the extremes would not over influence the results.

In summary, the increased risk of prostate cancer conferred by elevated levels of PhIP-DNA adducts in benign prostate tissue appears to be modest and confined to White men. However, the apparent dose–response nature of this relationship and its amplification in men with longer follow-up lends credence to this result. Based on animal models of PhIP-induced carcinogenesis, synergies between elevated adduct levels and pre-neoplastic changes are biologically plausible. Clearly, if PhIP is acting as a prostate carcinogen in humans, significant risk of cancer from PhIP exposure is likely confined to the subset of men with greater capacity to activate PhIP. Further study of determinates of PhIP metabolism in humans, and the role of inflammation in this process, is needed to identify men that may be at greatest risk for PhIP-induced carcinogenesis.

Acknowledgements

The authors thank the medical record abstractors and other study personnel that helped with data collection for this study. The authors especially thank Travis Wheeler and Nancy Lemke who processed all prostate specimens used in this study.

References

1. Felton JS, Knize MG, Shen NH, et al. The isolation and identification of a new mutagen from fried ground beef: 2-amino-1-methyl-6-phenylimidazo[4,5-b]pyridine (PhIP). *Carcinogenesis* 1986;7:1081–6.
2. Shirai T, Sano M, Tamano S, et al. The prostate: a target for carcinogenicity of 2-amino-1-methyl-6-phenylimidazo[4,5-b]pyridine (PhIP) derived from cooked foods. *Cancer Res* 1997;57:195–8.
3. Nakai Y, Nelson WG, De Marzo AM. The dietary charred meat carcinogen 2-amino-1-methyl-6-phenylimidazo[4,5-b]pyridine acts as both a tumor initiator and promoter in the rat ventral prostate. *Cancer Res* 2007;67:1378–84.
4. Shirai T, Kato K, Futakuchi M, et al. Organ differences in the enhancing potential of 2-amino-1-methyl-6-phenylimidazo[4,5-b]pyridine on carcinogenicity in the prostate, colon and pancreas. *Mutat Res* 2002;506–507:129–36.
5. Cui L, Takahashi S, Tada M, et al. Immunohistochemical detection of carcinogen-DNA adducts in normal human prostate tissues transplanted into the subcutis of athymic nude mice: results with 2-amino-1-methyl-6-phenylimidazo[4,5-b]pyridine (PhIP) and 3,2'-dimethyl-4-aminobiphenyl (DMAB) and relation to cytochrome P450s and N-acetyltransferase activity. *Jpn J Cancer Res* 2000;91:52–8.
6. Li G, Wang H, Liu AB, et al. Dietary carcinogen 2-amino-1-methyl-6-phenylimidazo[4,5-b]pyridine-induced prostate carcinogenesis in CYP1A-humanized mice. *Cancer Prev Res* 2012;5:963–72.
7. Wang CY, Debiec-Rychter M, Schut HA, et al. N-Acetyltransferase expression and DNA binding of N-hydroxyheterocyclic amines in human prostate epithelium. *Carcinogenesis* 1999;20:1591–5.
8. Williams JA, Martin FL, Muir GH, et al. Metabolic activation of carcinogens and expression of various cytochromes P450 in human prostate tissue. *Carcinogenesis* 2000;21:1683–9.
9. Malfatti MA, Felton JS. N-glucuronidation of 2-amino-1-methyl-6-phenylimidazo[4,5-b]pyridine (PhIP) and N_hydroxy-PhIP by specific human UDP-glucuronosyltransferases. *Carcinogenesis* 2001;22:1087–93.
10. Di Paolo OA, Teitel CH, Nowell S, et al. Expression of cytochromes P450 and glutathione S-transferases in human prostate, and the potential for activation of heterocyclic amine carcinogens via acetyl-coA-. *Int J Cancer* 2005;117:8–13.
11. Rybicki BA, Neslund-Dudas C, Bock CH, et al. Red wine consumption is inversely associated with 2-amino-1-methyl-6-phenylimidazo[4,5-b]pyridine-DNA adduct levels in prostate. *Cancer Prev Res (Phila)* 2011;4:1636–44.
12. Tang D, Liu JJ, Rundle A, et al. Grilled meat consumption and PhIP-DNA adducts in prostate carcinogenesis. *Cancer Epidemiol Biomarkers Prev* 2007;16:803–8.
13. Tang D, Liu JJ, Bock CH, et al. Racial differences in clinical and pathological associations with PhIP-DNA adducts in prostate. *Int J Cancer* 2007;121:1319–24.
14. Kooiman GG, Martin FL, Williams JA, et al. The influence of dietary and environmental factors on prostate cancer risk. *Prostate Cancer Prostatic Dis* 2000;3:256–8.
15. El-Zein R, Etzel CJ, Lopez MS, et al. Human sensitivity to PhIP: a novel marker for prostate cancer risk. *Mutat Res* 2006;601:1–10.
16. Punnen S, Hardin J, Cheng I, et al. Impact of meat consumption, preparation, and mutagens on aggressive prostate cancer. *PLoS One* 2011;6:e27711.
17. Major JM, Cross AJ, Watters JL, et al. Patterns of meat intake and risk of prostate cancer among African-Americans in a large prospective study. *Cancer Causes Control* 2011;22:1691–8.
18. Koutros S, Cross AJ, Sandler DP, et al. Meat and meat mutagens and risk of prostate cancer in the Agricultural Health Study. *Cancer Epidemiol Biomarkers Prev* 2008;17:80–7.
19. John EM, Stern MC, Sinha R, et al. Meat consumption, cooking practices, meat mutagens, and risk of prostate cancer. *Nutr Cancer* 2011;63:525–37.
20. Sander A, Linseisen J, Rohrmann S. Intake of heterocyclic aromatic amines and the risk of prostate cancer in the EPIC-Heidelberg cohort. *Cancer Causes Control* 2011;22:109–14.
21. Cross AJ, Peters U, Kirsh VA, et al. A prospective study of meat and meat mutagens and prostate cancer risk. *Cancer Res* 2005;65:11779–84.
22. Zhu J, Chang P, Bondy ML, et al. Detection of 2-amino-1-methyl-6-phenylimidazo[4,5-b]-pyridine-DNA adducts in normal breast tissues and risk of breast cancer. *Cancer Epidemiol Biomarkers Prev* 2003;12:830–7.
23. Zhu J, Rashid A, Cleary K, et al. Detection of 2-amino-1-methyl-6-phenylimidazo [4,5-b]-pyridine (PhIP)-DNA adducts in human pancreatic tissues. *Biomarkers* 2006;11:319–28.
24. Kryvenko ON, Jankowski M, Chitale DA, et al. Inflammation and preneoplastic lesions in benign prostate as risk factors for prostate cancer. *Mod Pathol* 2012;25:1023–32.
25. Takahashi S, Tamano S, Hirose M, et al. Immunohistochemical demonstration of carcinogen-DNA adducts in tissues of rats given 2-amino-1-methyl-6-phenylimidazo[4,5-b]pyridine (PhIP): detection in paraffin-embedded sections and tissue distribution. *Cancer Res* 1998;58:4307–13.
26. Lin D, Kaderlik KR, Turesky RJ, et al. Identification of N-(Deoxyguanosin-8-yl)—2-

amino-1-methyl-6-phenylimidazo [4,5-b]pyridine as the major adduct formed by the food-borne carcinogen, 2-amino-1-methyl-6-phenylimidazo[4,5-b]pyridine, with DNA. *Chem Res Toxicol* 1992;5:691–7.
27. Takahashi S, Hasegawa R, Mutai M, et al. Additive action of five heterocyclic amines in terms of induction of GST-P positive single cells and foci in rat liver-correlation with DNA adduct formation. *J Toxicol Pathol* 1994;7:423–8.
28. Bogen KT, Keating GA. U.S. dietary exposures to heterocyclic amines. *J Expo Anal Environ Epidemiol* 2001;11:155–68.
29. Nowell S, Ratnasinghe DL, Ambrosone CB, et al. Association of SULT1A1 phenotype and genotype with prostate cancer risk in African-Americans and Caucasians. *Cancer Epidemiol Biomarkers Prev* 2004;13:270–6.
30. Kidd LC, Stillwell WG, Yu MC, et al. Urinary excretion of 2-amino-1-methyl-6-phenylimidazo[4,5-b]pyridine (PhIP) in White, African-American, and Asian-American men in Los Angeles County. *Cancer Epidemiol Biomarkers Prev* 1999;8:439–45.
31. Kriek E, Rojas M, Alexandrov K, et al. Polycyclic aromatic hydrocarbon-DNA adducts in humans: relevance as biomarkers for exposure and cancer risk. *Mutat Res* 1998;400:215–31.
32. Gammon MD, Santella RM, Neugut AI, et al. Environmental toxins and breast cancer on Long Island. I. Polycyclic aromatic hydrocarbon DNA adducts. *Cancer Epidemiol Biomarkers Prev* 2002;11:677–85.
33. van Schooten FJ, Hillebrand MJ, van Leeuwen FE, et al. Polycyclic aromatic hydrocarbon—DNA adducts in white blood cells from lung cancer patients: no correlation with adduct levels in lung. *Carcinogenesis* 1992;13:987–93.
34. Wiencke JK, Kelsey KT, Varkonyi A, et al. Correlation of DNA adducts in blood mononuclear cells with tobacco carcinogen-induced damage in human lung. *Cancer Res* 1995;55:4910–4.
35. Sinha R. An epidemiologic approach to studying heterocyclic amines. *Mutat Res* 2002;506–507:197–204.
36. Norrish AE, Ferguson LR, Knize MG, et al. Heterocyclic amine content of cooked meat and risk of prostate cancer. *J Natl Cancer Inst* 1999;91:2038–44.
37. Relling MV, Lin JS, Ayers GD, et al. Racial and gender differences in N-acetyltransferase, xanthine oxidase, and CYP1A2 activities. *Clin Pharmacol Ther* 1992;52:643–58.
38. Malfatti MA, Felton JS. Human UDP-glucuronosyltransferase 1A1 is the primary enzyme responsible for the N-glucuronidation of N-hydroxy-PhIP in vitro. *Chem Res Toxicol* 2004;17:1137–44.
39. Girard H, Thibaudeau J, Court MH, et al. UGT1A1 polymorphisms are important determinants of dietary carcinogen detoxification in the liver. *Hepatology* 2005;42:448–57.
40. Girard H, Butler LM, Villeneuve L, et al. UGT1A1 and UGT1A9 functional variants, meat intake, and colon cancer, among Caucasians and African-Americans. *Mutat Res* 2008;644:56–63.
41. Knize MG, Kulp KS, Salmon CP, et al. Factors affecting human heterocyclic amine intake and the metabolism of PhIP. *Mutat Res* 2002;506–507:153–62.
42. Malfatti MA, Dingley KH, Nowell-Kadlubar S, et al. The urinary metabolite profile of the dietary carcinogen 2-amino-1-methyl-6-phenylimidazo[4,5-b]pyridine is predictive of colon DNA adducts after a low-dose exposure in humans. *Cancer Res* 2006;66:10541–7.
43. Wang W, Bergh A, Damber JE. Morphological transition of proliferative inflammatory atrophy to high-grade intraepithelial neoplasia and cancer in human prostate. *Prostate* 2009;69:1378–86.
44. Sfanos KS, De Marzo AM. Prostate cancer and inflammation: the evidence. *Histopathology* 2012;60:199–215.
45. Abdel-Razzak Z, Loyer P, Fautrel A, et al. Cytokines down-regulate expression of major cytochrome P-450 enzymes in adult human hepatocytes in primary culture. *Mol Pharmacol* 1993;44:707–15.
46. Sterling KM, Jr, Cutroneo KR. Constitutive and inducible expression of cytochromes P4501A (CYP1A1 and CYP1A2) in normal prostate and prostate cancer cells. *J Cell Biochem* 2004;91:423–9.
47. Murray GI, Taylor VE, McKay JA, et al. The immunohistochemical localization of drug-metabolizing enzymes in prostate cancer. *J Pathol* 1995;177:147–52.
48. Martin FL, Cole KJ, Muir GH, et al. Primary cultures of prostate cells and their ability to activate carcinogens. *Prostate Cancer Prostatic Dis* 2002;5:96–104.
49. Sakr WA, Grignon DJ, Crissman JD, et al. High grade prostatic intraepithelial neoplasia (HGPIN) and prostatic adenocarcinoma between the ages of 20–69: an autopsy study of 249 cases. *In Vivo* 1994;8:439–43.
50. Nonn L, Ananthanarayanan V, Gann PH. Evidence for field cancerization of the prostate. *Prostate* 2009;69:1470–9.
51. Keating GA, Bogen KT. Estimates of heterocyclic amine intake in the US population. *J Chromatogr B Analyt Technol Biomed Life Sci* 2004;802:127–33.
52. Keating GA, Bogen KT. Methods for estimating heterocyclic amine concentrations in cooked meats in the US diet. *Food Chem Toxicol* 2001;39:29–43.
53. Sinha R, Rothman N, Salmon CP, et al. Heterocyclic amine content in beef cooked by different methods to varying degrees of doneness and gravy made from meat drippings. *Food Chem Toxicol* 1998;36:279–87.
54. Gu D, Turesky RJ, Tao Y, et al. DNA adducts of 2-amino-1-methyl-6-phenylimidazo[4,5-b]pyridine and 4-aminobiphenyl are infrequently detected in human mammary tissue by liquid chromatography/tandem mass spectrometry. *Carcinogenesis* 2012;33:124–30.
55. Magagnotti C, Pastorelli R, Pozzi S, et al. Genetic polymorphisms and modulation of 2-amino-1-methyl-6-phenylimidazo[4,5-b]pyridine (PhIP)-DNA adducts in human lymphocytes. *Int J Cancer* 2003;107:878–84.

Cancer Science
The official journal of the Japanese Cancer Association

Apocynin, an NADPH oxidase inhibitor, suppresses rat prostate carcinogenesis

Shugo Suzuki,[1,2,5] Kazuhide Shiraga,[1] Shinya Sato,[1] Wanisa Punfa,[1,3] Aya Naiki-Ito,[1] Yoriko Yamashita,[1] Tomoyuki Shirai[1,4] and Satoru Takahashi[1]

[1]Department of Experimental Pathology and Tumor Biology, Nagoya City University Graduate School of Medical Sciences, Nagoya; [2]Pathology Division, Nagoya City East Medical Center, Nagoya, Japan; [3]Department of Biochemistry, Faculty of Medicine, Chiang Mai University, Chiang Mai, Thailand; [4]Nagoya City Rehabilitation Center, Nagoya, Japan

(Received July 12, 2013/Revised September 6, 2013/Accepted September 19, 2013/Accepted manuscript online September 30, 2013/Article first published online October 28, 2013)

Recent evidence suggests that oxidative stress contributes to the pathogenesis of prostate cancer. The present study focused on the effect of apocynin, an inhibitor of NADPH oxidase, on prostate carcinogenesis using the transgenic rat for adenocarcinoma of prostate (TRAP) model. There were no toxic effects with apocynin treatment. The percentages and numbers of carcinomas in both the ventral and lateral prostate were significantly reduced by apocynin treatment, with dose dependence. Reduction of reactive oxygen species by apocynin was confirmed by immunohistochemistry of 8-OHdG and dihydroethidium staining. Positivity of Ki67 was significantly reduced by apocynin treatment, and downregulation of clusterin expression, as well as inactivation of the MEK-ERK1/2 pathway, was a feature of the apocynin treated groups. In human prostate cancer cell line LNCaP, apocynin also inhibited reactive oxygen species production and blocked cell growth by inducing G0/G1 arrest with downregulation of clusterin and cyclin D1. These data suggest that apocynin possesses chemopreventive potential against prostate cancer. (*Cancer Sci* 2013; 104: 1711–1717)

Prostate cancer is the second most frequently diagnosed cancer in men in the world, with particularly high incidences in Oceania, Europe and North America. In Japan, incident and mortality rates for prostate cancer are relatively low are but increasing.[1,2] There are potentially curative options, such as radical prostatectomy or radiotherapy, but once the disease is metastatic, the outlook is poor. Therefore, research into chemoprevention of prostate cancer is critical.

Reactive oxygen species (ROS) can be important factors for carcinogenesis and tumor progression, not only inducing DNA damage but also producing cellular alterations, such as upregulation of MAPK and protein kinase C.[3,4] Recently, oxidative stress has been reported to contribute to cancer and progression in the prostate.[5,6] Therefore, we have focused on inhibition of ROS production as an anti-carcinogenic approach. ROS is produced by mitochondria, peroxisomes, cytochrome P-450 and other cellular elements as a byproduct, and is generated by NADPH oxidase, which is also implicated in a variety of signaling events, including cell growth, cell survival and cell death.[7] Apocynin, which belongs to the methoxy-substituted catechol family, inhibits NADPH oxidase activity by blocking the formation of NADPH oxidase complex[8] and is commonly used as a standard NOX inhibitor for research purposes.[7] In addition, apocynin can be converted by peroxidase-mediated oxidation to a dimer, which has been shown to be a more efficient inhibitor than apocynin itself.[9] We previously presented evidence that apocynin reduced oxidative stress induced by arsenite treatment of rat urothelium *in vivo*.[10]

In the present study we focus on NADPH oxidase and test whether its inhibitor, apocynin, is able to suppress prostate carcinogenesis in the transgenic rat for adenocarcinoma of prostate (TRAP) model, which was generated in our laboratory and features development of well-differentiated prostate adenocarcinomas in prostatic lobes within a short period. The TRAP rat has a transgene that encodes SV40 T antigen under probasin promoter, so that the carcinomas that develop are androgen-dependent.[11,12]

Materials and Methods

Animal experiment. Male heterozygous TRAP rats established in our laboratory with a Sprague–Dawley genetic background were used in the present study. All animals were housed in plastic cages on wood-chip bedding in an air-conditioned specific pathogen-free animal room at 22 ± 2°C and 55 ± 5% humidity with a 12 h light/dark cycle, and fed a basal diet (Oriental MF, Oriental Yeast, Tokyo, Japan) and provided water, with or without apocynin, *ad libitum*. All animal experiments were performed under protocols approved by the Institutional Animal Care and Use Committee of Nagoya City University School of Medical Sciences.

Six-week-old TRAP rats were divided into three groups of 11 rats each. The animals were given drinking water containing 0, 100 and 500 mg/L apocynin for 8 weeks and body weight and water consumption were estimated every week. At experimental week 8, under deep isoflurane anesthesia, blood was collected from 9.00 to 11.00 h to measure testosterone and estradiol hormone levels using radioimmunoassays from a commercial laboratory (SRL, Tokyo, Japan). Adiponectin concentrations in serum were determined by ELISA (adiponectin ELISA kit; Otsuka Pharmaceutical, Tokyo, Japan). The urogenital complex of each rat was removed as a whole together with the seminal vesicles, then the ventral prostate was weighed. A part of the prostate glands was immediately frozen in liquid nitrogen and stored at −80°C until processed. After that, the remaining tissue was fixed. Livers, kidneys and testes were also removed, weighed and fixed. For clusterin immunostaining, normal prostate glands from a 14-week-old male Sprague–Dawley rat were fixed. The tissues were routinely processed into paraffin-embedded sections and stained with H&E.

Histopathology and immunohistochemistry. Neoplastic lesions in the prostate gland of TRAP rats were evaluated as previously described.[13,14] Briefly, neoplastic lesions were classified into three types: low grade prostatic intraepithelial neoplasia (LG-PIN), high grade PIN (HG-PIN) and adenocarcinoma. The relative numbers of acini with the histological

[5]To whom correspondence should be addressed.
E-mail: shugo@med.nagoya-cu.ac.jp

doi: 10.1111/cas.12292

characteristics of each type, that is, LG-PIN, HG-PIN and adenocarcinoma, were quantified by counting the total acini in each prostatic lobe. Deparaffinized sections were incubated with diluted antibodies for Ki-67 (Novocastra Laboratories, Newcastle, UK), anti-8-hydroxy-2′-deoxyguanosine (8-OHdG) antibody (Japan Institute for the Control of Aging, Fukuroi, Japan), clusterin (Santa Cruz Biotechnology, Santa Cruz, CA, USA), androgen receptor (AR) and SV40 T antigen (Santa Cruz Biotechnology). The number of Ki-67-labeled or 8-OHdG-labeled cells in at least 1000 cells was counted to determine the labeling indices of HG-PIN and adenocarcinoma.

Detection of reactive oxygen species production. Six-micron frozen serial sections cut on a standard cryostat with clean blades were mounted on slides, then incubated with 5 μM dihydroethidium (Life Technologies, Carlsbad, CA, USA) in PBS for 15 min in the dark. The slides were washed two times with warm PBS and the fluorescence intensity was assessed at 518/605 nm with a spectrofluorometer. Images were also recorded with a fluorescence microscope (BZ-9000; Keyence, Osaka, Japan).

Microarray analysis. Total RNA was isolated from ventral prostate tissues en bloc by phenol–chloroform extraction (ISOGEN, Nippon Gene, Toyama, Japan). Gene expression analysis was performed using a Rat Oligo chip 20k (Toray Industries, Tokyo, Japan) according to the manufacturer's instructions. The RNA ventral prostate expression from 500 mg/L apocynin-treated rats was compared with that from control rats. After global median normalization, data cleansing was performed to remove the values for which fluorescence intensity was <100. The genes for which expression were more than twofold increased or reduced to less than half in 500 mg/L apocynin-treated rats as compared to control rats were selected.

Real-time RT-PCR. Total RNAs from ventral prostate tissues were reverse-transcribed with the ThermoScript first-strand synthesis system (Life Technologies), and real-time RT-PCR was performed using a LightCycler (Roche Diagnostics GmbH, Penzberg, Germany). The quantitative value of clusterin was normalized to endogenous cyclophilin. Clusterin RT-PCR primers were 5′-TTATGGACACAGTGGCAGAG-3′ and 5′-TACAGAACCCAGAGGAAGGA-3′. Cyclophilin RT-PCR primers were 5′-TGCTGGACCAAACACAAATG-3′ and 5′-GAAGGGGAATGAGGAAAATA-3′.

Immunoblot analyses. Ventral prostate tissues were homogenized with RIPA buffer (Pierce Biotechnology, Rockford, IL, USA) containing a protease inhibitor (Pierce Biotechnology) on ice. The insoluble matter was removed by centrifugation at 10 000*g* for 20 min at 4°C and supernatants were collected. Protein concentrations were determined with a Coomassie Plus – The Better Bradford Assay Kit (Pierce Biotechnology). Samples were mixed with 2× sample buffer (Bio-Rad Laboratories, Hercules, CA, USA) and heated for 5 min at 95°C and then subjected to SDS-PAGE. The separated proteins were transferred onto nitrocellulose membranes followed by blocking with SuperBlock Blocking Buffer (Thermo Fisher Scientific, Waltham, MA, USA) for 1 h at room temperature. Membranes were probed with antibodies for cyclin D1, clusterin, cleaved caspase-3, MEK, phospho-MEK, p44/42 MAPK (ERK1/2), phopho-ERK1/2, p38 MAPK, phospho-p38 MAPK, and caspase 3 and 7 (Cell Signaling Technology, Danvers, MA, USA) in 1× TBS with 0.1% Tween 20 at 4°C overnight, followed by exposure to peroxidase-conjugated appropriate secondary antibodies and visualization with an enhanced chemiluminescence detection system (GE Healthcare Bio-sciences, Buckinghamshire, NA, UK). To confirm equal protein loading, each membrane was stripped and reprobed with anti-β-actin (Sigma-Aldrich, St. Louis, MO, USA).

Cell line. The human androgen-dependent prostate cancer cell line LNCaP was obtained from the American Type Culture Collection (Manassas, VA, USA). The cells were grown in RPMI1640 medium with 10% FBS, 100 U/mL penicillin and 100 μg/mL streptomycin (all from Life Technologies) under an atmosphere of 95% air and 5% CO_2 at 37°C.

Cell proliferation assay. Cell proliferation of prostate cancer cell lines was assessed by 4-[3-(4-iodophenyl)-2-(4-nitrophenyl)-2H-5-tetrazolio]-1,3-benzene disulfonate tetrazolium salt (WST-1) assay (Roche Applied Science, Mannheim, Germany). Briefly, cells were seeded in 96-well plates at 500 cells/well in 200 μL of culture medium. Apocynin was added 24 h after seeding and incubated for 3 days. WST-1 reagent was added to each well with incubation for 60 min at 37°C, and then each well was measured for absorbance at 430 nm.

Detection of reactive oxygen species production in LNCaP cells. The culture supernatant was removed from all wells 24 h after apocynin treatment, and the cells were washed twice with warm PBS, then 2′,7′-dichlorofluorescin-diacetate (100 μg/mL, DCFH-DA, Sigma-Aldrich) was added with further incubation at 37°C for 20 min, in the dark. The cells were washed two times with warm RPMI1640 medium, and images were recorded using a fluorescence microscope (BZ-9000; Keyence).

Cell cycle analysis. Cells were treated with apocynin for 24 h, then suspensions were prepared and stained with propidium iodide (Guava Cell Cycle Reagent, Guava Technologies, Hayward, CA, USA) according to the Guava Cell Cycle Assay protocol. Cell cycle phase distributions were determined on a Guava PCA Instrument using CytoSoft Software.

Statistical analysis. All *in vitro* experiments were performed at least in triplicate to confirm reproducibility. Statistical analyses were performed with mean ± SD values using one-way ANOVA and Dunnett's test. Statistical significance was concluded at $*P < 0.05$, $**P < 0.01$ or $***P < 0.001$.

Results

Apocynin reduction of progression of prostate tumorigenesis as well as cell proliferation and reactive oxygen species in TRAP rats. During the experiments, water consumption by 500 mg/L apocynin-treated rats was approximately 10% lower than in the controls (Table 1). However, administration of apocynin did not cause adverse effects (e.g. impacting the growth of rats) during the study. There were no significant differences in the final body weights or in absolute and relative liver,

Table 1. Body and organ weights, water consumption

Treatment	Number of rats	Body weight (g)	Liver (g)	Kidneys (g)	Testes (g)	Ventral prostate (g)	Water consumption (mL/rat/day)
Control	11	533 ± 58	18.5 ± 2.0	3.2 ± 0.2	3.5 ± 0.4	0.30 ± 0.06	45.5 ± 4.4
100 mg/L	11	553 ± 49	20.1 ± 2.3	3.1 ± 0.3	3.6 ± 0.3	0.36 ± 0.09	46.5 ± 5.5
500 mg/L	11	558 ± 65	20.2 ± 3.2	3.2 ± 0.4	3.6 ± 0.4	0.30 ± 0.04	39.6 ± 2.6*

*Significantly different from control group, $P < 0.05$.

doi: 10.1111/cas.12292

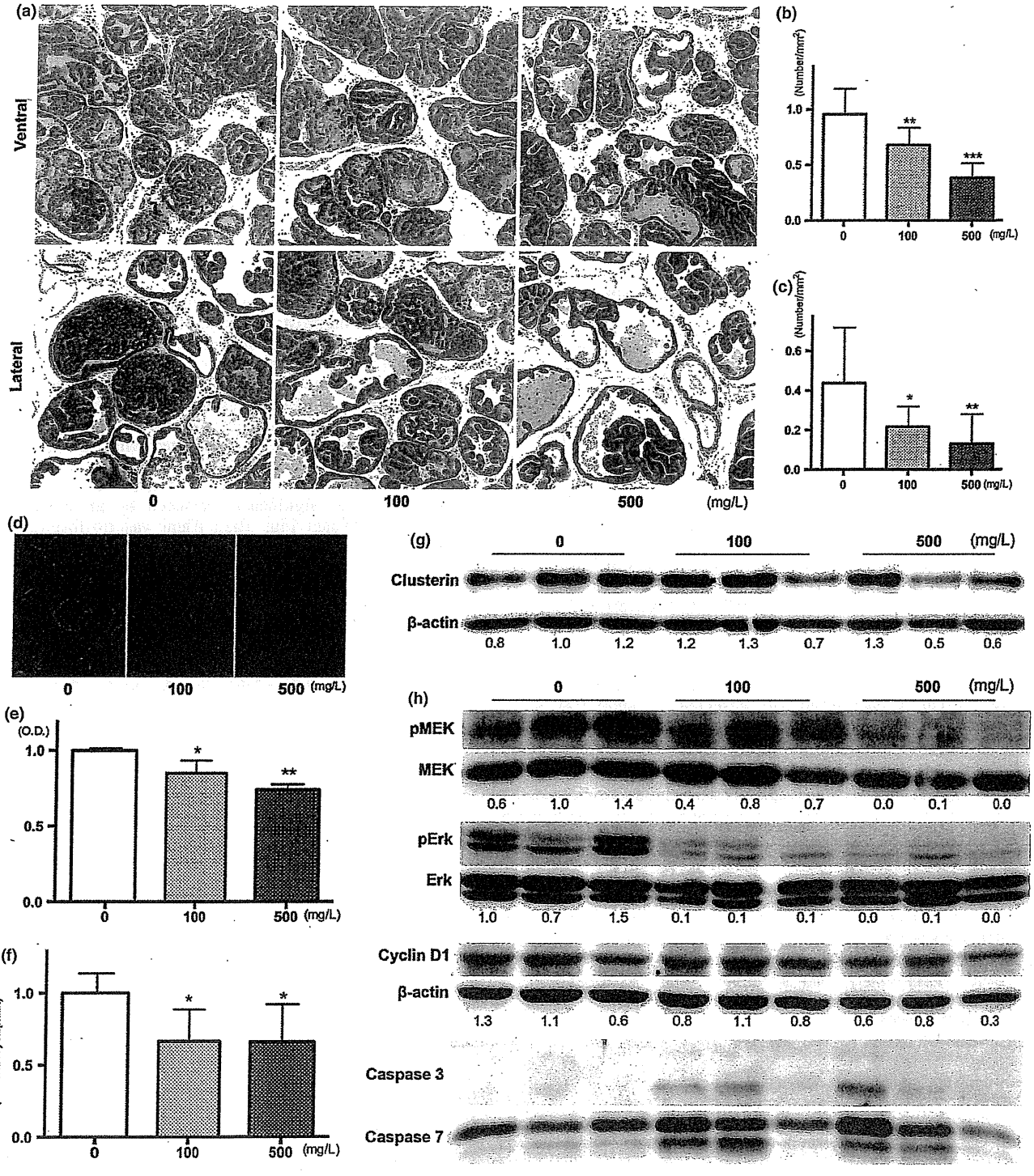

Fig. 1. Effects of apocynin on prostatic lesions. Representative histopathological findings for lesions in the ventral and lateral prostates of the controls, 100 and 500 mg/L apocynin groups (a). Number of adenocarcinoma per area in ventral (b) and lateral (c) prostate of TRAP rats treated with apocynin. Photos (d) and data (e) for reactive oxygen species production detected by dihydroethidium staining in ventral prostate of TRAP rats treated with apocynin. Expression of clusterin detected by quantitative RT-PCR (f) and western blotting (g). Results of immunoblot analysis of MAPK, cyclin D1 and caspases in ventral prostates of TRAP rats treated with apocynin. Data are mean ± SD values from 3 independent experiments. *,**,***$P < 0.05$, 0.01 and 0.001 compared to controls, respectively.

kidney, testes and prostate weights among the groups (Table 1). Histologically, there were no changes indicative of toxicity in the liver, kidneys, and testes with apocynin (data not shown). The serum level of testosterone in 500 mg/L apocynin treated rats (3.1 ± 1.6 ng/mL) was slightly higher than in other groups (control and 100 mg/L apocynin: